Your thesaurus codes are:
05 (08.01.1; 11.01.1; 11.05.2; 11.13.1; 11.19.4; 11.19.5)

ASTROPHYSICS
April 5, 2000

Age and metallicity for six LMC clusters and their surrounding field population

B. Dirsch[1], **T. Richtler**[2], **W.P. Gieren**[2], **M. Hilker**[3]

[1] Sternwarte der Universität Bonn, Auf dem Hügel 71, 53121 Bonn, Germany
[2] Universidad de Concepción, Departamento de Física, Casilla 160-C, Concepción, Chile
[3] P. Universidad Católica, Departamento de Astronomía y Astrofísica, Casilla 104, Santiago 22, Chile

the date of receipt and acceptance should be inserted later

Abstract. We investigate, on the basis of CCD Strömgren photometry, the ages and metallicities of six LMC clusters together with their surrounding field population. The clusters and metallicities are: NGC 1651 (in the range $[Fe/H] = -0.65$ dex to -0.41 dex), NGC 1711 (-0.57 ± 0.17 dex), NGC 1806 (-0.71 ± 0.23 dex), NGC 2031 (-0.52 ± 0.21 dex) and NGC 2136/37 (-0.55 ± 0.23 dex) and NGC 2257 (-1.63 ± 0.21 dex). The metallicities for NGC 1651, NGC 1711, NGC 1806 and NGC 2031 have been determined for the first time (NGC 2031 and NGC 2136/37 are interesting for the Cepheid distance scale).

In the cluster surroundings, we found about 650 field stars that were suitable to be used for a determination of an age-metallicity relation (AMR). Our method is to estimate ages for individual stars on the basis of Strömgren isochrones with individually measured metallicities. With this method we are able to sample the AMR of the field population up to 8 Gyr.

Our metallicity data are incompatible with models predicting many metal-poor stars (G-dwarf problem). The metallicity of the field population increased by a factor of six, starting around 2 Gyr ago. The proposed AMR is consistent with the AMR of the LMC cluster system (including ESO 121 SC03 and three clusters with an age of 4 Gyr).

The proposed AMR is incompatible with the recently proposed AMR by Pagel & Tautvaišvienė (1998).

Key words: Stars: abundances - Galaxies: abundances, evolution, Magellanic Clouds, star clusters, stellar content

1. Introduction

In spite of its enormous importance for understanding galaxy evolution in adequate detail, the chemical enrichment process in galaxies is still poorly known, which is especially true for the field star component. The Large Magellanic Cloud (LMC) is a natural target to study the chemical evolution because of its proximity. Also, its structure seems to be less complex than that of the Milky Way which might imply that the chemical enrichment history can be described by a simple global age-metallicity relationship (AMR).

First efforts to determine the AMR of LMC clusters have been made with integrated broad band photometry of clusters (Westerlund 1997). Recent work continuing these studies is, for example, Bica et al. (1998) and Girardi et al. (1995). Another major step towards an understanding of the LMC cluster AMR has been undertaken by Olszewski et al. (1991), who used medium resolution spectroscopy of individual giants to measure the metallicity for around 70 clusters, with a quoted uncertainty of ± 0.2 dex. In addition many photometric studies of stars in LMC clusters (e.g. with the Washington system by Bica et al. 1998) contributed to the unveiling of the cluster AMR.

The current wisdom on the cluster AMR that has been established by these studies is, that the mean metallicity of younger clusters is distinctly higher than that of old clusters by more than 1.2 dex. However, it is difficult to trace the AMR over the entire LMC history with this cluster sample, since for a long time, only one cluster (ESO121-SC03) with an age between 3 Gyr and 11 Gyr had been found (Mateo et al. 1986, Bica et al. 1998). Recently, Sarajedini (1998) found three more clusters with an age of about 4 Gyr (NGC 2121, NGC 2155 and SL 663).

The AMR as derived from LMC clusters shows a very large scatter (Olszewski et al. 1991), which, if intrinsic and not due to measurement uncertainties, would argue for a more complex chemical enrichment history. In addition there are hints that at least some clusters have smaller mean metallicities than the surrounding field population (e.g. Bica et al. 1998, Richtler et al. 1989). Thus possibly the chemical evolution of the cluster and field stars is to some degree decoupled. However, this is not without contradiction (e.g. Korn et al. 2000). Santos Jr. et al. (1999) claimed that the metallicity dispersion of the field seems to be smaller than that of the cluster system of similar age.

For the field population the metallicity distribution is known primarily for the young stars since mainly F & G supergiants have been spectroscopically investigated (e.g. Hill et al. 1995, Luck & Lambert 1992, Russell & Bessell 1989). A compilation of young LMC field stars abundances which have been

Send offprint requests to: bdirsch@astro.uni-bonn.de

derived with high resolution spectroscopy can be found in the appendix (Table A4). Thévenin & Jasniewicz (1992) study 9 field stars in the LMC with medium resolution spectroscopy (5 $\AA$) and found an average abundance of $[Fe/H] = -0.25 \pm 0.08$ which is higher than the mean value of field stars that has been derived with high resolution spectroscopy (-0.38 ± 0.11 dex). Dopita et al. (1997) measured element abundances of planetary nebulae (PNs) in the LMC and derived their age by modelling the hot, central star. They found four PNs that are older than 4 Gyr. Their AMR shows only little enrichment from 15 to 5 Gyr ago, while the metallicity doubled in the last $2-3$ Gyr. The study of the older stellar field component has been limited to studies using broad band photometry (e.g. Holtzman et al. 1999 and Elson et al. 1997).

We used a different approach and measured the metallicity of individual stars by using the medium wide Strömgren filter system, that gives a good metallicity discrimination for giants and supergiants red-wards of $b-y = 0.4$ mag. This method has already been used by Grebel & Richtler (1992), Hilker et al. (1995b) and Hilker et al. (1995a) to determine age and metallicity of NGC 330, NGC 1866 and NGC 2136/37. Ardeberg et al. (1997) used HST observations transformed into the Strömgren system to derive the SFH and the metallicity of LMC bar stars. Their investigation differs from our approach by the calibration they employed which is based on bluer stars and includes the gravity dependent $c1$ Strömgren colour index.

In the current work we investigate mainly young LMC clusters and their surrounding fields, namely NGC 1651, NGC 1711, NGC 1806, NGC 2031, and NGC 2257, an old cluster. We have also re-analysed NGC 2136/37 because of the availability of Strömgren isochrones and a new calibration for photometric metallicities, which improves the calibration for more metal poor stars. This ensures the homogeneity of the sample and also tests if systematic shifts are present between the older investigations and the new one. An important aspect of this new work is exactly this homogeneity of the metallicities allowing one to assess the real magnitude of the intrinsic dispersion among metallicities of clusters of similar age.

Two of the clusters (NGC 2136 and NGC 2031) are particularly interesting because they contain Cepheid variables, whose metallicities are important to know for distance scale problems. NGC 1866 might serve as example. Its metallicity has been determined by Hilker et al. (1995b) via Strömgren photometry which was used for the distance determination using its Cepheid members by Gieren et al. (1994).

2. Data & Reduction

The data have been obtained during two observing runs with the 1.54-m Danish telescope at La Silla, Chile. NGC 2136 and NGC 2031 were observed during 13.11. - 15.11.1992, and NGC 1651, NGC 1711, NGC 1806, NGC 2257 during 4.1. - 7.1.1994. The observing log is shown in Table A1 in the Appendix. We used the UV coated Thomson THX 31560 chip, that has a field of view of $6.5' \times 6.5'$ and a scale of 0.377″/pixel. The Danish imaging Strömgren filters v, b and y were used.

Table 1. Coordinates of the investigated clusters

Cluster	α_{2000}	δ_{2000}	l	b
NGC 1651	$4^h37^m12^s$	$-70^0 33''$	282.75^0	-36.42^0
NGC 1711	$4^h50^m36^s$	$-69^0 59''$	281.61^0	-35.57^0
NGC 1806	$5^h2^m11^s$	$-67^0 03''$	278.89^0	-35.16^0
NGC 2031	$5^h33^m36^s$	$-70^0 59''$	281.73	-31.85^0
NGC 2136	$5^h53^m17^s$	$-69^0 32''$	279.83	-30.35^0
NGC 2257	$6^h30^m24^s$	$-64^0 17''$	274.10	-26.51^0

The measurements in these filters have been transformed into a Johnson V magnitude, the colour $b-y$ and the colour index $m1 = (v-b)-(b-y)$.

Except for NGC 1711 each cluster has been observed on at least two different nights to have photometrically independent measurements. The reduction included bias subtraction, flat-field correction and the elimination of CCD defects. We used DaoPhot II in the MIDAS and IRAF environments for the photometry.

For the calibration we employed six different E-region standard stars from the list of Jønch-Sørensen (1993) and four fields with secondary Strömgren standards measured by Richtler (1990), namely M 67, SK -66 80, NGC 2257 and NGC 330. The heavily crowded field of NGC 330 with the secondary standards measured with photoelectric photometry is problematic since slight differences in centring the aperture on a standard star lead to deviations in the obtained magnitude on the order of 0.02 mag. Thus several stars in this field have been removed from the calibration. The photometric error of a single measurement is given by the standard deviation of the standard stars: $\sigma_y = 0.031$, $\sigma_{b-y} = 0.028$ and $\sigma_{m1} = 0.036$. We obtained the errors by averaging the residuals of the calibration stars in all nights. The calibration errors for the 1992 run are smaller: $\sigma_y = 0.016$, $\sigma_{b-y} = 0.023$ $\sigma_{m1} = 0.025$. However, since standard stars are always measured in the central region of the CCD chip, this error does not include flat-field errors which are much harder to quantify (especially also due to the problematic field concentration in telescopes with focal reducers (Andersen et al. 1995). From inspection of the sky background the accuracy of the flat-field is $\simeq 1-2\%$ and we therefore assigned an additional error of 0.015 to each magnitude. The photometric standards were measured with apertures and thus it was necessary to determine the aperture - PSF shift carefully. The remaining uncertainty is of the order of 0.03 mag. Even if several nights have been averaged this calibration error has been kept, since the calibrations in each night are not truly independent: the colour terms have been determined using the standard star observations from all nights together. Thus we overestimated the calibration error for the clusters by a factor $< \sqrt{nights}$ if observations from several nights have been averaged.

The calibration error causes the deviation of the measured metallicity from the "true" metallicity of a star to be a function of its colour (shown in Fig. 1). The corresponding metallicity error is larger for blue stars since lines of constant metallicity approach each other on the blue side (see Fig. 5 for illustration).

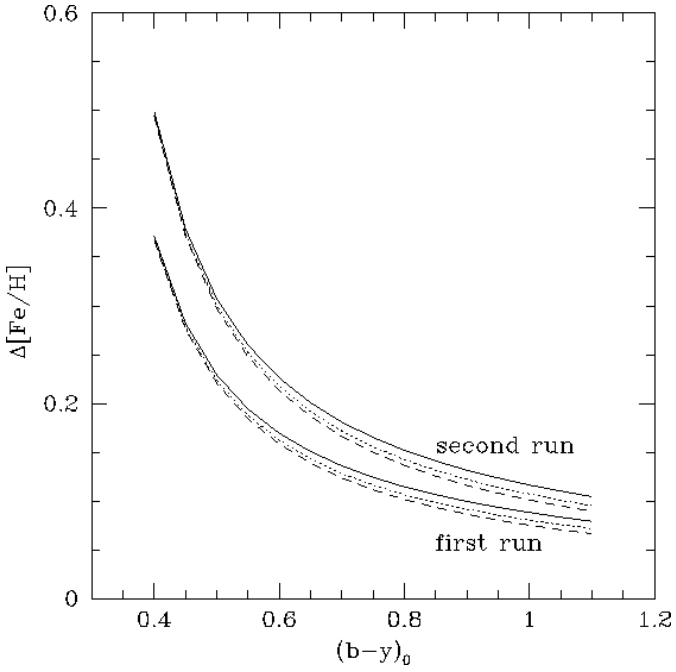

Fig. 1. The calibration error results in an error of the measured metallicity that depends on the colour of the star. In this graph we plotted the metallicity error due to this calibration error versus the star's colour, each curve sample corresponds to one run (1994 & 1992). Lines are drawn for 0, -1 and -2 dex stars (solid lines, short dashed lines, long dashed lines)

In the following stars bluer than $b-y=0.6$ are excluded from the metallicity determination because of this strong rise of the metallicity uncertainty.

3. Metallicity determination via Strömgren colours

The major advantage of the Strömgren system compared to broad band photometric systems is the ability to get the metallicity of a star nearly independent of its age The reason for this independence is the minor luminosity effect in the metallicity determination, which amounts to less than ± 0.1 dex over a luminosity interval of $-4 < M_V < 3$.

We have used a new metallicity calibration of the Strömgren $m1-(b-y)$ two-colour relation by Hilker (1999) which is valid in the colour range $0.5 < b-y < 1.1$. For redder stars the calibration breaks down due to the onset of absorption by TiO and MgH molecules in the y band. The used calibration equation is

$$\left[\frac{Fe}{H}\right] = \frac{m1_0 + a1\cdot(b-y)_0 + a2}{a3\cdot(b-y)_0 + a4}$$

with

$$a1 = -1.277 \pm 0.050,\ a2 = 0.331 \pm 0.035$$
$$a3 = 0.324 \pm 0.035,\ a4 = -0.032 \pm 0.025$$

This calibration has been derived using primarily giant stars, however as investigated by Grebel & Richtler (1992) it should also apply to supergiants. For stars bluer $b-y=0.7$ this has been predicted by Gustafsson & Bell (1979). We will discuss this question in greater detail in Sect. 3.4.

The reason for the metal sensitivity is the line blocking in the v filter, which is best measurable for G and K stars. The measured flux depends largely on the strength of the Fe I lines, but also CN and CH bands contribute. Systematic deviations of less than 0.1 dex are expected from theoretical isochrones due to a small luminosity dependence.

3.1. The CN anomaly

A severe problem in the interpretation of Strömgren colours is the contribution of the CN molecule absorption (band head at 421.5 nm) in the v-filter (410 nm, width 20 nm) to the line blocking. CN variations have been observed in several galactic globular clusters, however, the exact mechanism is not yet fully understood. An increased CN abundance leads to an increased photometric metallicity and thus to a decreased age if it is derived via isochrones. As a rule of thumb we estimated with the aid of Geneva isochrones that an increased metallicity of 0.2 dex will decrease the age by $\approx 20\%$. A recent investigation using Strömgren photometry of two globular clusters, of which one has CN anomalous stars, the other not, illustrates the effect of CN anomaly on the Strömgren metallicity (Richter et al. 1999).

We cannot account for this CN anomaly. In this study we have to live with this uncertainty, but there is evidence that this effect is only modest: in the nearby giant sample (see next section) three stars were assigned to be CN enriched, but they do not deviate within the standard deviation from the CN-normal stars, however most probably due to the uncertain reddening correction. Pilachowski et al. (1996) found that for population II halo stars the CN anomaly does not play an important role, in contrast to M 13 for example. This cannot be explained by simple selection effects. Mc Gregor & Hyland (1984) found a general CN deficiency by weaker CO bands in the LMC than in galactic supergiants of the same temperature. Concerning our LMC field stars we found a good agreement for the young stars with spectroscopic analyses as well as for the older field population with observed clusters (see below). Therefore anomalous CN abundances should not play a devastating role. Ultimately this can only be checked with a spectroscopic investigation of the CN behaviour of cool LMC giants and supergiants.

3.2. The influence of reddening uncertainties

Photometrically measured metallicities are very sensitive to reddening errors, which is a major error source of the determined metallicities. For example an underestimation of the reddening of 0.02 mag in E_{b-y} leads to an average underestimation of the metallicity by $\Delta[Fe/H]=0.1$ dex for a fully populated RGB with an age around $10^{9.0}$ yr. This problem is symptomatic for photometric investigations. For example Bica et al. (1998) who used Washington photometry to derive ages and metallicities of old LMC clusters and the field, stated that "*an*

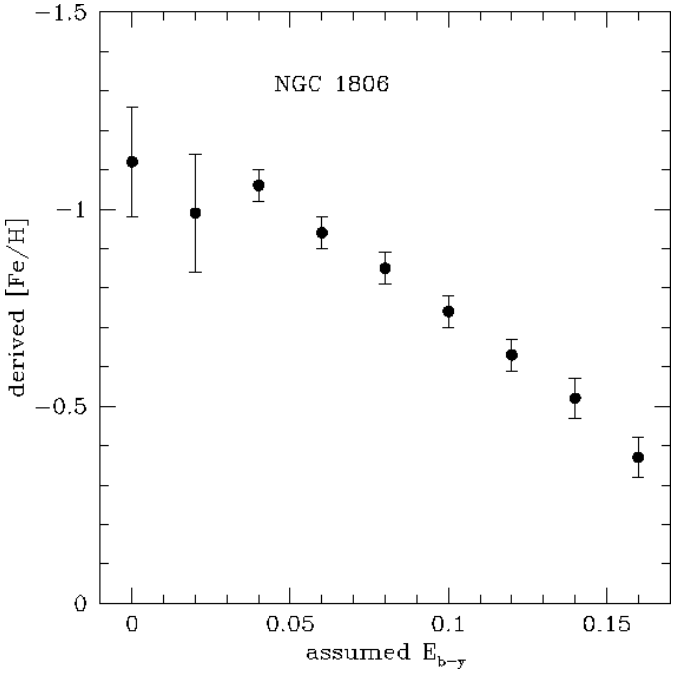

Fig. 2. The metallicity of NGC 1806 derived from the $m1$,$(b-y)$ diagram is plotted as a function of the applied reddening. The errors have been derived by dividing the standard deviation of the mean metallicity with the square-root of the number of stars used for the metallicity determination.

increase of the assumed reddening by E(B-V)=0.03 decreases the derived metallicity by 0.12 dex". The degeneracy between reddening and abundance becomes a severe problem for old clusters and field stars, while for young clusters it is possible to determine the reddening quite accurately because the colour of the hot, bright main sequence stars is nearly independent of temperature and thus of metallicity. The dependence of the derived metallicity on the assumed reddening is illustrated in Fig. 2, with NGC 1806 as an example (we note that this figure greatly exaggerates the realistic uncertainty of the reddening for this particular cluster and just serves to illustrate the trend).

Differential reddening is another aspect of this problem. We cannot exclude it, however there are also no hints in favour of strong differential reddening. Olsen (1999) investigated four fields in the LMC (three in the bar, one in the inner disk), where the reddening is expected to be larger than in our further outside lying fields. However, they detected strong differential reddening only around NGC 1916. For the other fields it is not significant.

We estimated with the aid of Monte Carlo simulations, that as long as the differential reddening is less than $E_{B-V} = 0.03$ (peak to peak), the uncertainty is small compared to the photometric uncertainty. In any case differential reddening results in a broadening of the metallicity and hence the age distribution.

3.3. Unresolved binaries and blending

The observation of unresolved binaries, which is likely to be the case for a considerable fraction of stars, leads to a change in the photometric metallicity. Fortunately this effect plays a negligible role for stars on the RGB where the mass-luminosity relation is steep and even small differences in the initial mass result in large differences in luminosity. This has been checked with the aid of synthetic CMDs and two-colour diagrams, which is described in Sect. 12 below.

In crowded fields blending of stars is a related problem which is nicely illustrated in Fig. 1 in the work of Ardeberg et al. (1997). The first correction is to exclude the most crowded inner part of the clusters thus we excluded stars within $\approx 19''$ from the cluster center (details in the cluster sections). The most probable, but unimportant, case is blending with a faint, red main sequence star: they are not luminous enough to change the photometric metallicity of a RGB star. To estimate the probability of blending with other stars we used the following approach: we assumed that blending takes place if the luminosity centres of gravity of two stars are nearer than the PSF radius divided by $\sqrt{2}$ (sampling theorem). Since the PSF radius was always around 3 pixels the area in which only one unblended star can be is $(2 \cdot 3/\sqrt{2})^2 \cdot \pi$. Next we counted the stars on the blue and red side of the observed CMD (bluer and redder than $(b-y) = 0.4$) in luminosity intervals fainter than the main star and calculated the probability that one of these fainter stars lie within the area of the main component. We label the blending with a star "strong blending", if the luminosity difference of this star and the main component is less than 2 mag. Blending with a star that is between 2 and 4 magnitudes fainter is called "weak blending" and corresponds to a luminosity ratio of at least 6 that results in shifts of < 0.2 dex. The probability of weak blending is underestimated since incompleteness has not been considered. However, weak blending primarily results in a broadening of the metallicity distribution of < 0.15 dex. Also the strong blending is slightly underestimated since a truly blended star is counted in the observed CMD only once, but since the probability for strong blending is well below 10% (see below) we regard this approximation to be justified for our fields. Blending with a main sequence star results in a shift of the combined pair towards bluer colour and and smaller m1. The shift in $(b-y)$ dominates and thus the resulting metallicity is in general larger for this pair than for the individual RGB star. Very strongly blended stars even leave the selected colour range and thus our selection also ensures the exclusion of heavily blended stars.

The fields of NGC 1711 and NGC 1806 shall serve as examples for the expected blending probability. These fields are rather crowded compared to the fields around NGC 1651, NGC 2257 and NGC 2136, but comparable with the crowding around NGC 2031. The strong blending probability with a blue main sequence star decreases from 8% for a 18.5 mag RGB star to less than 1% for a 15 mag star in the field of NGC 1711. The probability for strong blending with a red star decreases from 3% to $< 1\%$. Around NGC 1806 the strong blending with red

stars is more probable: it decreases from 10% to $< 1\%$ for a luminosity of the main component between 18.5 mag and 15 mag. The probability of weak blending is for a 17 mag RGB stars $\approx 10\%$ around NGC 1806 and $\approx 5\%$ around NGC 1711. We conclude that $\approx 5\%$ of our selected stars have a Strömgren metallicity that deviates by more than 0.2 dex from its "true" value due to blending. Around 10% of the stars are blended with a resulting shift of < 0.2 dex.

The deviations in age due to blending are more difficult to determine: on the one hand the increasing luminosity would result in an underestimation of the age, on the other hand for strong blending with a blue star, the metallicity would be underestimated, which generally leads to an overestimation of the age. We conclude that also for the age, blending results primarily in a broadening of the age distribution, however, with a distribution that is more extended towards younger ages, i.e. it is more probable to underestimate than to overestimate the age (this has been found with the aid of the mentioned simulation). In the discussion in Sect. 14 we will give an additional argument that the blending in clusters result in shifts of less than 0.1 dex compared to the field, assumed that cluster and field population of the same age have the same metallicity based on the observations.

3.4. AGB versus RGB stars

AGB stars are in the age range of $10^{8.4}$ yr to $10^{9.0}$ yr the dominating giant stars. These stars are potentially problematic since their surface abundances might have changed considerably compared to the initial composition. However, in M 13 Pilachowski et al. (1996) found that the AGB stars are less CN enriched than the RGB stars.

Frogel & Blanco (1990) identified several AGB stars around some of our clusters, for which Olszewski et al. (1991) obtained the metallicity. However, these stars are always too red to allow a photometric metallicity determination.

3.5. Are the Strömgren metallicities independent of the luminosity class?

The re-calibration of the Strömgren metallicity of red stars by Hilker (1999) is based on giant stars for the lower metallicity range and approach the calibration of Grebel & Richtler (1992) for higher metallicities (however also below 0 dex). In the earlier work by Grebel & Richtler (1992) no difference between giant and supergiant stars has been found. ¿From the theoretical point of view, only a very small luminosity effect is expected (Bell & Gustafsson 1978 and the used isochrones by Grebel & Roberts 1995a).

To reinvestigate observationally the dependence of the Strömgren metallicity on the luminosity class, we selected supergiants (luminosity class I & II) with metallicity measurements and Strömgren photometry from the compilation of Cayrel de Strobel et al. (1997) and SIMBAD, respectively. The major problem of this approach is the largely unknown reddening towards these galactic field supergiants. To exclude stars that are most probable highly reddened we took only supergiants with a galactic latitude $|l| > 20^0$ and brighter than 6 mag in V into account. The remaining supergiants are shown in Fig. 3, where the difference of the Strömgren metallicity to the measured metallicity (taken from the list of Cayrel de Strobel et al. 1997) versus the measured metallicity is displayed. Fig. 3 open circles are used for variable stars, and open star symbols for carbon stars and stars with a CN anomaly. We did not attempt to correct for the individual reddening, which explains partially the considerable scatter. The vertical lines shows the location of the literature metallicity of -0.1 dex and the horizontal line indicates where spectroscopic and photometric metallicities are equal.

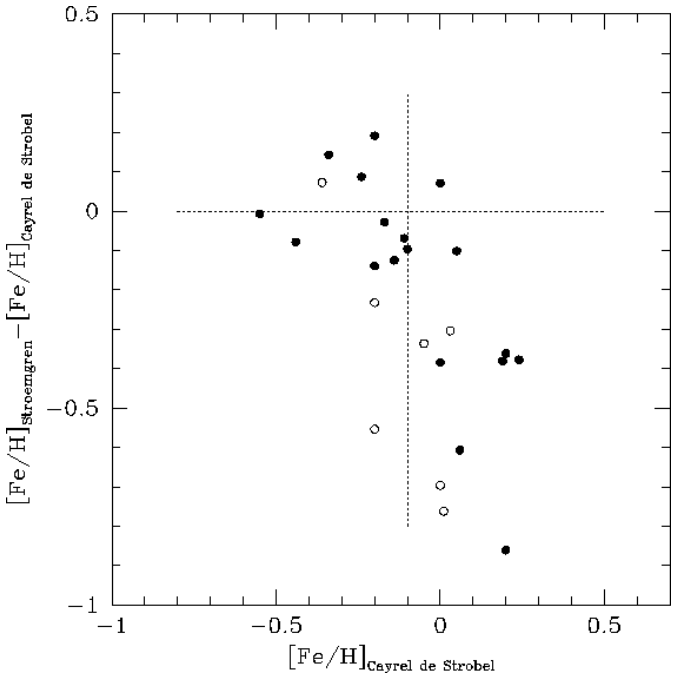

Fig. 3. Difference between the Strömgren metallicity of galactic supergiants (luminosity class I & II) and the metallicities given by Cayrel de Strobel (1997). Solid dots denote "normal" stars while open dots are used for variable supergiants. The reddening correction employed is $E_(B-V) = 0.03$. With such a small average reddening the metallicity difference of the normal stars which are metal poorer than 0 dex is $\Delta[Fe/H] = -0.01 \pm 0.12$ dex.

It can be seen in Fig. 3 that the calibration seems to hold for supergiants with a metallicity of less than -0.1 dex (we have corrected for a systematic shift of -0.1 dex which can easily be explained with an average reddening of $E_{B-V} = 0.02$). For larger metallicities the Strömgren metallicities seem to underestimate the "true" metallicity. However, the calibration has been made only for stars of subsolar metallicity, thus the deviation of more metal rich stars is not surprising.

4. The age determination

To determine ages of stars and clusters we employed isochrones provided by the Geneva (Schaerer et al. 1993) and Padua (Bertelli et al. 1994) groups transformed into the

Strömgren system by Grebel & Roberts (1995a); they are called "Geneva" and "Padua" isochrones in the following. The isochrones show a zero point difference to the empirical calibration in the sense that an isochrone of a given metallicity is too red and/or $m1$ is too low compared to the calibration, which is of the order of 0.15 dex. To solve this discrepancy we increased the $m1$ values of the isochrones by 0.04 mag to bring them into accordance with the empirical calibration. We have chosen the $m1$ colour index, since it contains the v filter, which is the most critical one in the filter-band integration of the model spectra due to it's fairly short wavelength. For this central wavelength the applied stellar atmospheres of red giants and supergiants are not very precise (Bressan priv. comm.). Unfortunately, only Geneva isochrones with metallicities of more than -1.4 dex and ages of less than $10^{9.9}$ yr were available. Padua isochrones on the other hand covered only the age range between $10^{7.0} - 10^{9.0}$ yr and $10^{10.0} - 10^{10.24}$ yr, thus most of our results are based on the Geneva isochrones.

The very red part of the RGB is not red enough to describe the location of the observed RGB stars correctly, the isochrones are slightly too steep for $(B - V) > 1.1$. With the observed RGBs of NGC 1651, NGC 1806 and the field surrounding NGC 1711, we introduced an empirical linear colour term to bring the isochrones into agreement with these stars (for $(b - y) > 0.7$ the applied shift is: $0.6 \cdot ((b - y) - 0.7)$, the maximum correction is $\Delta(b-y) = 0.12$). After we applied this correction the isochrones fit also to the younger clusters, which is a hint that the colour term is valid for all gravities. However, nothing can be said for old stars ($> 10^{9.5}$ yr) since no clear RGB with such an age was available to test the empirical colour term (NGC 2257 is too metal poor and too old for this purpose). The $m1$ had to be changed according to the colour term in $b - y$, which has been performed on the basis of the empirical metallicity calibration.

The isochrones show a small age-metallicity degeneracy: a substantial age difference between a $10^{7.5}$ yr and a $10^{9.9}$ yr isochrone leads only to a difference in the photometric metallicity of $\Delta[Fe/H] = 0.2$, in the sense that younger stars would appear more metal rich. Since we adjusted a $10^{9.0}$ yr isochrone (via the $m1$ shift) to the empirical metallicity calibration, the resulting metallicity uncertainty is less than 0.1 dex. Throughout the paper we assumed a distance modulus of 18.5 for the LMC based on surface brightness analysis of Cepheids (Gieren et al. 1998), results from SN1987A (Panagia et al. 1991) and on the recent revision of the "classical" Cepheid distance calibration (Madore & Freedman 1998). A distance uncertainty has a direct effect on the age determination in the sense that a smaller distance to the LMC would result in lower ages.

5. Selecting cluster and field stars

5.1. Cluster stars

The first step in measuring the metallicity of a cluster is to separate its members from the surrounding field population. We performed this mainly by selecting stars within a certain radial distance from the cluster. The selection radius is defined as the radius where the cluster star density starts to be higher than 2σ over the background star density, which has been derived with a radial density profile of the stars in the frame. The innermost part ($< 20''$) of the clusters has been excluded because it is impossible to derive reliable photometry for stars in this crowded region, especially due to blending.

For young clusters also the luminosity of a star is a good criterion to separate cluster and field stars, since it is easy to distinguish bright, young cluster stars from old field RGB stars. Clearly this criterion does not separate field and cluster stars of similar age. The lower luminosity limit that was used to exclude RGB field stars in this approach has been determined by visual inspection of the CMD. It is straightforward for NGC 1711, NGC 2031 and NGC 2136/37, where the cluster stars are much brighter than the field RGB, however, this criterion could not be applied for NGC 1651, NGC 1806 and NGC 2257.

We did not perform a statistical field star subtraction for two reasons: we wanted to have the most reliable cluster stars and including stars from a larger radius might lead to a bias towards field stars that have a similar age and metallicity, since the statistical field star subtraction has to work in chunks of colour and luminosities. If the colour and luminosity range of the bins in which the field stars are subtracted are chosen too small than the Poisson error is large, if they are chosen too large, then the resulting distribution is not "cleaner" than the one in our approach. Moreover, since the numbers of stars are frequently much smaller than for the field population, the error in the number of stars would heavily depend on the field star population, especially if the incompleteness varies strongly with radial distance from the cluster. This varying incompleteness would lead to a considerable uncertainty. The disadvantage of our approach is certainly that there will always be some field stars left.

Stars with a photometric error (DaoPhot) of more than $\Delta(b - y) = 0.1$ and $\Delta m1 = 0.1$ have been discarded. This selection ensures more reliable results.

Finally, only stars redder than $(b - y)_0 = 0.6$ have entered the metallicity measurement to reduce the systematic shifts in the derived metallicity due to a possible error in the applied reddening correction, which is illustrated in Fig. 2. Also stars being redder than $(b - y) = 1.1$ have been discarded due to additional lines in the y filter.

From the remaining sample, individual stars have been excluded if they deviate strikingly from the mean metallicity or from the mean RGB location of the other stars, because still a few field and foreground stars might be present, as mentioned above.

5.2. Field stars

Field stars have been selected with a radial selection criterion as well: we regard as field stars those with a radial distance of more than $30''$ plus the radius used for selecting the corresponding cluster The additional $30''$ have been added to ensure

Table 2. Expected foreground stars (Ratnatunga & Bahcall 1985) per $44(')^2$ (the size of our CCD field) for the LMC.

V	$(b-y)<0.4$	$0.5<(b-y)<0.8$	$(b-y)<0.8$
$13-15$	1.3	0.7	0.1
$15-17$	4	3.4	0.7
$17-19$	4	7.0	5.0
$19-21$	8.4	5.7	17.2

To transform $(B-V)$ into the Strömgren $(b-y)$ we used $(B-V) = -0.055 + 1.707(b-y)$, that has been derived with the available isochrones.

that cluster stars are a minor fraction among the field stars. Only field stars with a relative photometric error of less than $\Delta(b-y) = 0.1$ and $\Delta m1 = 0.1$ have been kept. In case of the young clusters NGC 1711, NGC 2031 and NGC 2136/37 we used all RGB stars having a distance of more than $70''$ from the cluster center, since they clearly do not belong to the cluster.

To minimise the influence of photometric and calibration errors on the derived metallicity, it is necessary to introduce the colour criterion $(b-y)_0 > 0.6$, as it has been done in the case of clusters. However, it is dangerous to limit the sample just in colour since this introduces a large bias towards metal poor stars with larger metallicity errors [1]. This is not a big problem for younger clusters, where the giants extend far into the red and therefore the metallicity measurement does not depend so severely on the blue stars. To circumvent this problem and to have nevertheless a reasonable homogeneous selection criterion, we included only stars that are redder than an inclined line in the $m1-(b-y)$ diagram that is nearly perpendicular to $[Fe/H] = -1$ dex, a metallicity which is in the middle of the expected metallicity range in the LMC. This line is shown for example in the two-colour plot of the field population around NGC 1711 (Fig. 7).

5.3. Galactic foreground stars

Foreground stars of our own Galaxy contaminate the field and cluster sample in the observed fields. Most of the foreground stars are red clump stars which show up as a broad vertical strip at $b-y \approx 0.4$. Ratnatunga & Bahacall (1985) presented a galaxy model and give the amount of galactic foreground stars in luminosity and colour bins. Their results are compiled in Table 2. With these numbers in mind it is obvious that we expect only few galactic foreground stars in the colour and luminosity range we used for the metallicity and age determination.

6. The reddening towards individual clusters and the surrounding field

Because of the large influence of the reddening on the measured metallicity, as described in Sect. 3, it is necessary to get a hand on the reddening correction towards the observed regions. For this purpose we used the theoretical upper main sequence ($(b-y)_0 < 0.1$ and $M_V < 0$) for the reddening determination, because of the negligible metallicity metallicity effects. It is essential not to fit the isochrone to the centre of the main sequence, since the isochrones are calculated for non-rotating stars and evolutionary effects on the upper main sequence. Rotation shifts a star redwards and thus one has to fit the isochrone more to the blue border of the observed main sequence. Also unresolved binaries on the main sequence are redder than the observed isochrones. However, since photometric errors are also present the fit of a blue envelope would be exaggerated.

For the extinction correction the relations of Crawford & Barnes (1970) have been employed ($E_{b-y} = 0.7E_{B-V}$ and $E_{m1} = -0.3E_{b-y}$). Since the reddening is derived on the assumption that the colour of the isochrone is correct for the very bright blue main sequence we only give the possible uncertainty in the adjustment of the isochrones to the main sequence as a reddening error. However, our reddening is always smaller than the reddening given by Schlegel et al. (1998), which is a hint that there is a zero point shift in $b-y$ between either our calibration or the isochrones on the order of $\Delta b-y = 0.03$. It might of course be a zero point shift in the Schlegel et al. values as well, especially when considering that the given reddening values are frequently larger than the one by other authors (see Sect. 6 - Sect. 11).

7. NGC 1711

7.1. The cluster

Several attempts have been made to determine the age of NGC 1711. One of them used also isochrone fitting (Sagar & Richtler 1991), however, with an *assumed* metallicity of -0.4 dex. The previous results on the age of NGC 1711 are compiled in Table A2 in the appendix. No metallicity measurement for this cluster has been published yet. The CMD of the entire CCD field is shown in Fig. A1.

Using the upper main sequence ($V < 18.5$) we have deduced a reddening of $E_{b-y} = 0.06 \pm 0.02$, relative to the isochrone, which corresponds to $E_{B-V} = 0.09 \pm 0.05$ (the calibration error has already been included). The determined reddening agrees, within the errors, with $E_{B-V} = 0.14$ given by Cassatella et al. (1996) and with the reddening derived from measurements by Schwering & Israel (1991) ($E_{B-V} = 0.11$). Burstein & Heiles (1982) gives $E_{B-V} = 0.12$.

Concerning the reddening, it is important to note that the surrounding field, where one can observe young stars with a similar age, shows a 0.02 mag higher reddening, indicating that NGC 1711 is located in front of the LMC disk. Fig. 4 illustrates this difference. This also holds for a small concentration of brighter stars south-east of NGC 1711. Unfortunately, the number of stars in this group is not large enough to allow a reliable age or metallicity determination. However, because of the same colour difference between field and cluster, it might

[1] $\Delta m1$ is the dominating error in the Strömgren two-colour diagram. Therefore, the metallicity error will be larger for more metal poor stars than for more metal rich stars of the same colour.

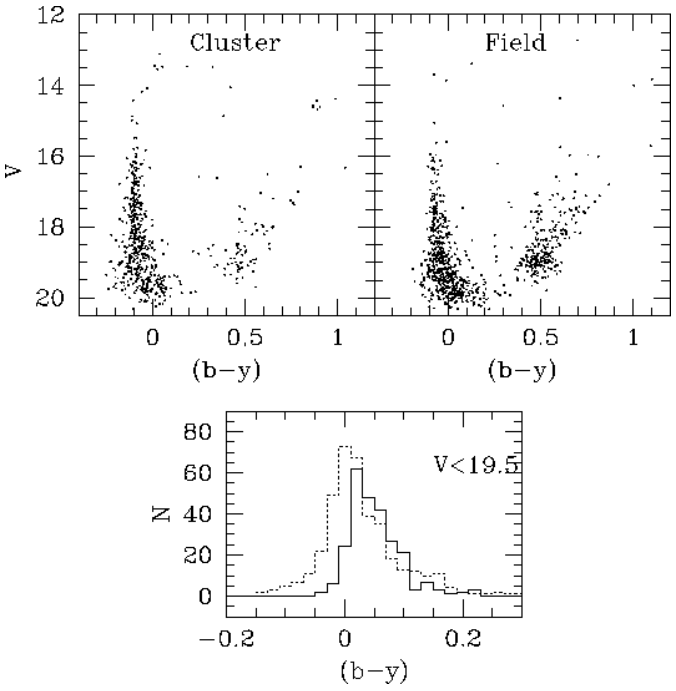

Fig. 4. Illustration of the reddening difference of 0.02 mag between NGC 1711 and its surrounding field stars. In the upper panel the CMDs of cluster and field are shown. In the lower panel the colour histogram of main sequence stars brighter than $V = 19.5$ mag are plotted with a dotted line for the cluster and with a solid line for the field. For illustrative purposes, the radial selection for the field was chosen to result in approximately the same number of field and cluster stars.

form a binary cluster with NGC 1711, a configuration, which seems to be common in the LMC [2] (e.g. Dieball & Grebel 1998 and references therein).

By inspecting the radial number density of stars around NGC 1711, we have found that cluster stars begin to dominate (2σ level) the field stars at a radial distance of $90''$. This radius has been used for the radial selection. To exclude older field RGB stars, we regarded only stars brighter than $V_0 = 15.5$ as potential cluster members for the metallicity analysis. The CMD and two-colour diagram of NGC 1711 is presented in Fig. 6 and Fig. 5, respectively. In the two-colour diagram we plotted the calibration error separately and assigned only the photometric error to the individual stars. The effect of these two errors is completely different: the metallicity error due to the photometric errors decrease with increasing size of the sample, while in contrast the metallicity error due to the calibration can only be decreased if observations from different nights are averaged.

We measured a metallicity of $[Fe/H] = -0.57 \pm 0.06$ dex for NGC 1711. The error is the standard deviation of the individual stars divided by the square root of the number of used stars (5). Reddening and calibration error account for an additional error of 0.16 dex, thus we finally obtained $[Fe/H] = -0.57 \pm 0.17$. To be able to fit the red supergiants one needs an isochrone with a metallicity of at least -0.4 dex, despite the measured metallicity. We showed in Sect. 3.2, that the calibration is valid for supergiants, as long as they have a metallicity below 0 dex. From Fig. 3 one could estimate that a supergiant with a metallicity around 0.2 dex could be mistaken for a -0.5 dex star. However, we prefer a different explanation: as described in Sect. 3, a slight age dependence exist accounting for ± 0.1 dex, in the sense that younger stars appear more metal poor. With this in mind we derived a metallicity of $[Fe/H] = -0.45 \pm 0.2$ (we assigned an additional error of 0.05 because of the uncertainty of the shift). A third possibility is that the isochrones does not sufficiently extend towards the red for these bright stars, despite the empirical correction. This is mainly a problem in the treatment of overshooting and a common problem for red supergiants (Bressan priv. comm.). We arrived at an age of $10^{7.70 \pm 0.05}$ yr using Geneva isochrones. The isochrone is overlayed in Fig. 6.

7.2. The surrounding field population

We used only bright ($V < 16$) stars that are more than $110''$ away from the cluster centre and all RGB stars with a distance of $> 50''$.

The field population consists of a main sequence slightly more reddened and an older population clearly distinguishable by its giant branch. A remarkable feature is the vertical extension of the red clump (VRC), which has been observed in other areas of the LMC as well. This has been interpreted by Zaritsky & Lin (1997) as a signature of an intervening population towards the LMC, but Beaulieu & Sacket (1998) showed that also normal stellar evolution could lead to such a feature, if a $10^{8.5}$ yr to $10^{9.0}$ yr old population is present. Even the fainter extension (or fainter second red clump), might be present (Girardi 1999, Piatti et al. 1999), however the numbers are definitely too small to allow an unambiguous identification.

With a reddening of $E_{B-V} = 0.11$ we can derive the metallicity of the field stars which is illustrated in Fig. 7. The average metallicity of the field population is $[Fe/H] = -0.53$ dex and the standard deviation 0.42 dex.

The unambiguously young field stars, which are marked with star symbols in Fig. 7 and Fig. 8, have a mean metallicity of -0.56 ± 0.27 which is not systematically larger than the one of the older population, even when accounting for the slight age dependence of the metallicity. Stars in the narrow metallicity range $-0.75 < [Fe/H] < -0.45$ (filled circles) do not exhibit a uniform age. An upper age limit of the field stars is $10^{8.9}$ yr. This means that between $10^{7.7}$ yr and approximately $10^{8.9}$ yr no clear age-metallicity dependence can be seen in this field.

8. NGC 1806

8.1. The cluster

NGC 1806 is older than NGC 1711, which can immediately be seen from its pronounced RGB (see Fig. 10). No previous CCD CMD is available in the literature. A faint main sequence of a younger field population is visible in the field

[2] 10% of the LMC clusters are thought to be paired

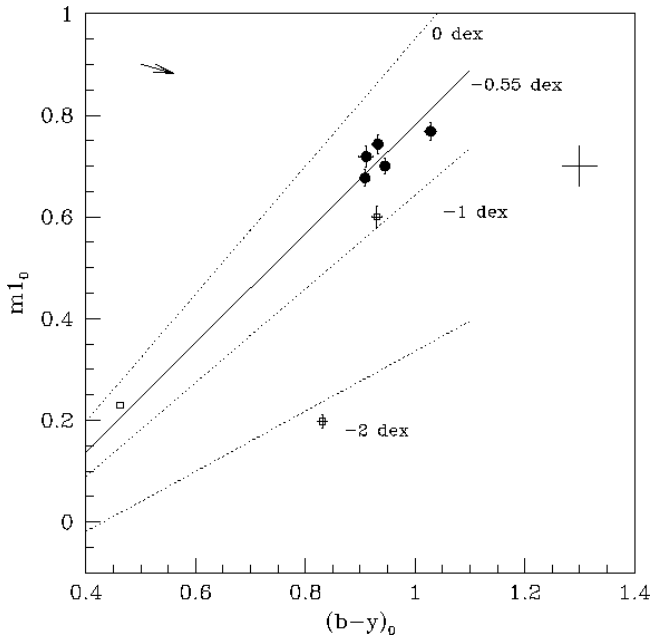

Fig. 5. Reddening corrected two-colour diagram for the stars selected in the CMD of NGC 1711 with a radial ($r < 90''$) and a luminosity criterion ($V < 15$). (Fig. 6). The open squares are used for excluded stars, while the filled circles show stars which entered the metallicity determination. The apparently metal poor star is most probable a Galactic halo foreground star. The cross at the right border shows the calibration error.

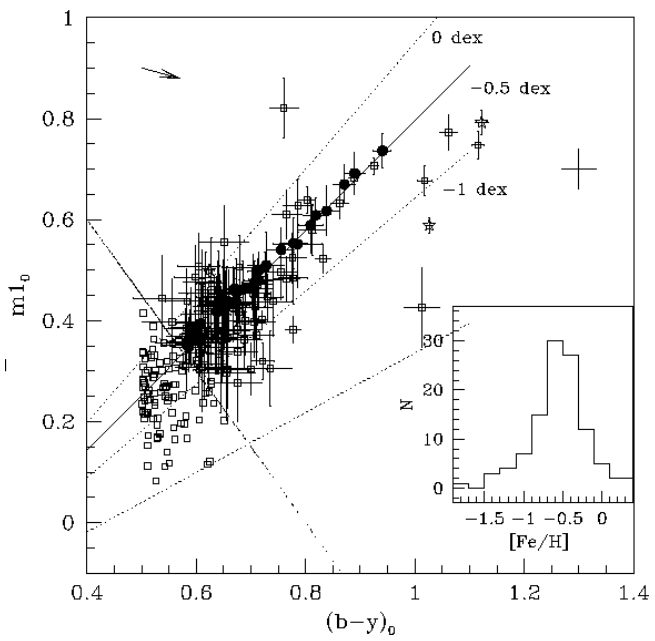

Fig. 7. Two-colour diagram for the stars which are further than $110''$ away from the cluster centre of NGC 1711. The inclined line from the upper left to the lower right marks the selection criterion applied to the colour: only stars redder than this line have been used to calculate the mean and standard deviation of the field star metallicity. The open squares redder than the selection line are stars fainter $V = 15$, the stars brighter than $V = 15$ are shown as open stars. Filled circles represent stars being fainter $V = 15$ and in the metallicity range $-0.75 < [Fe/H] < -0.45$. The other open squares mark all stars for which the calibration by Hilker (1999) is valid. The insert shows the metallicity distribution of all stars redder than the selection line.

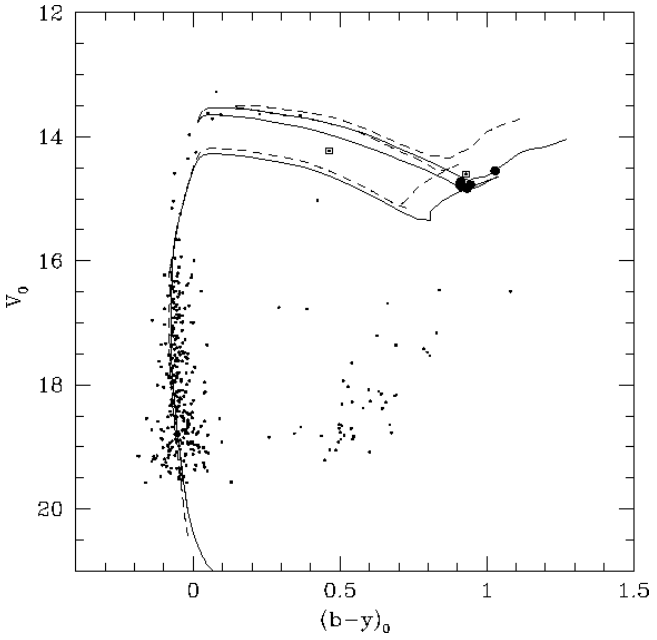

Fig. 6. CMD for the cluster area of NGC 1711. The symbols are the same as in Fig. 5. Geneva isochrones are overlaid with -0.4 dex (full line) and -0.7 dex (dashed line) with an age of $10^{7.7}$ yr.

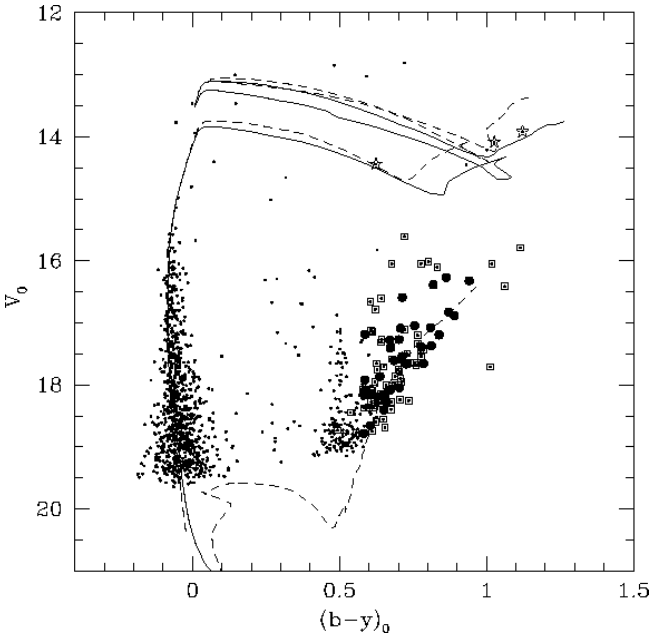

Fig. 8. CMD of the field stars around NGC 1711. Only stars redder than the colour selection line have been marked with symbols. The symbols are the same as those used in the two-colour diagram of the field stars (Fig. 7). The younger isochrones are Geneva isochrones with a metallicity of -0.4 dex and -0.7 dex and an age of $10^{7.6}$ yr, the older one has a metallicity of -0.7 dex and an age of $10^{9.2}$ yr.

around NGC 1806 (Fig. A1). This population has been used to determine a reddening of $E_{b-y} = 0.12 \pm 0.02$ ($E_{B-V} = 0.17 \pm 0.03$), which agrees, within the errors, with the values given by Cassatella et al. (1987) ($E_{B-V} = 0.12$). Schwering & Israel (1991) give $E_{B-V} = 0.10$ and Schlegel et al. (1998) $E_{B-V} = 0.24$. Burstein & Heiles (1982) derived a reddening of $E_{B-V} = 0.06$ towards this direction. We assumed that the cluster is reddened by the same amount as the field main sequence stars. The strong dependence of the derived metallicity on the reddening correction has been demonstrated for this cluster in Fig. 2.

Only stars within the radial distance of $60''$ have been taken for the metallicity determination. In addition, some stars lying apart from the average RGB location have been excluded. These stars are marked with open star symbols in the cluster CMD (Fig. 10). The inclusion of these stars would not change the derived metallicity.

We obtained a metallicity of $[Fe/H] = -0.71 \pm 0.06$ dex for NGC 1806. The calibration and reddening uncertainty result in an additional error of $\Delta[Fe/H] = \pm 0.23$ dex, hence $[Fe/H] = -0.7 \pm 0.24$ dex. The reddest cluster star (that has been excluded because of its red colour) is an identified AGB star (Frogel & Blanco 1990, LE 6), for which Olszewski et al. (1991) determined a metallicity of -0.7 dex, which is in good agreement with our value for this cluster.

The two-colour diagram is presented in Fig. 9. Some remarkable stars are those being redder $(b-y) = 1.0$ and apparently more metal poor than the other cluster stars. If these stars were members of a true metal poor population one would have expected to find bluer stars of the same metallicity, which is not the case. Because of this reason we think that these stars belong to NGC 1806, but they possess additional absorption lines in the y band compared to the bluer RGB stars. This is theoretically expected for red stars with solar metallicity, however the theoretical Geneva isochrones of this metallicity do not extend far into the red regime and no Padua isochrone with appropriate metallicity and age has been available. ¿From the identified AGB star one might speculate that these deviating stars are AGB stars in NGC 1806, which is supported by the best fitting isochrone (see below).

The age determination is illustrated in Fig. 10. The best fitting isochrone yields an age of $10^{8.7\pm0.1}$ yr. This is much younger than the age of $10^{9.6\pm0.1}$ yr derived by Bica et al. (1996) using the SWB classification. The red branch of this isochrone consists mainly of AGB stars especially in the employed colour range for the metallicity determination.

8.2. The surrounding field population

The metallicity of the field population has been derived with all stars that have a distance of at least $100''$ from the cluster centre. With the above stated reddening the mean metallicity of the field population can be obtained as -0.67 dex with a (relatively small) standard deviation of 0.23 dex.

A feature that is visible in the two-colour diagram of NGC 1806 (Fig. 11) is that stars that are redder than $b-y \simeq 1$ seem not to follow a straight line for a given metallicity, but rather get smaller $m1$ values with increasing $b-y$. The deviation is of the order -0.5 dex. This behaviour is similar to what is observed among the cluster stars of NGC 1806. Again, we argue that these stars might deviate from the line of constant metallicity given by the calibration. If these stars belong to a true metal-poor population one would expect to find more metal-poor stars with a colour between $0.9 < (b-y)_0 < 1.1$; this is not the case. No star is found in the whole colour range with a metallicity of lower than -1.3 dex, while four stars are found in an even smaller colour range of $\Delta(b-y) = 0.1$. Therefore, one would expect to find at least eight stars in the bluer colour range when assuming a homogeneously populated RGB, which is not unreasonable since the bottom part of a RGB around this age usually is even more populated than the upper part of the RGB. These peculiar red stars could be foreground stars as well, however it is intriguing that they are mixed with the other RGB stars in the CMD. Therefore we think that they belong to the LMC. Thus we reconfirm the statement that even low metallicity stars are only good tracers for metallicity as long as they are bluer than $b-y = 1.1$.

9. NGC 2136/37

9.1. The cluster

NGC 2136/37 is a potential triple cluster system (Hilker et al. 1995a) and thus another example of the common multiplicity among LMC clusters. The main components have an angular separation of $1'.34$. We have re-investigated this cluster due to the availability of Strömgren isochrones and because of the new calibration. NGC 2136 contains at least eight Cepheids making the knowledge of its metallicity particularly interesting for the Cepheid distance scale and the metallicity dependence of the PLC relation. The Cepheids have not been included in the derivation of the metallicity.

After the inspection of the radial number distribution of stars around the cluster centre we selected all stars with a distance of less than $75''$. Additionally we excluded probable RGB stars of the field population with $V > 16.5$.

The reddening can be determined with the upper main sequence and we obtained $E_{b-y} = 0.07 \pm 0.02$ ($E_{B-V} = 0.10 \pm 0.03$). This agrees with the reddening of $E_{B-V} = 0.09$ given by Schwering & Israel (1991). Burstein & Heiles (1982) obtained a reddening of $E_{B-V} = 0.075$.

The resulting metallicity of NGC 2136 is $[Fe/H] = -0.55 \pm 0.06$ dex (see Fig. 13). Two stars have been excluded, one metal rich one with solar metallicity and a metal poor one with ≈ -1 dex. The more metal rich star is most probably a binary star or the centre of a background galaxy, since its χ^2 value given by the DaoPhot PSF fitting routine is worse than for stars with comparable luminosity. The more metal poor star might be a remaining field star. The stars used for the metallicity determination are shown together with the $[Fe/H]$ histogram in Fig. 13. Including the calibration and reddening error we got -0.55 ± 0.23 dex. This is the same value as Hilker et al. (1995a) one obtained.

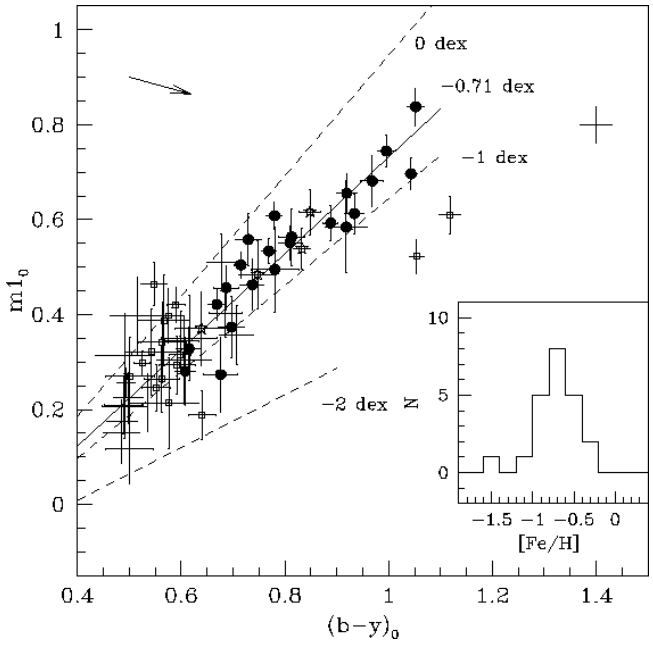

Fig. 9. Two-colour diagram of NGC 1806. The filled circles refer to stars with a distance of less than $60''$ from the cluster centre. In addition to the usual selection criteria we have excluded stars that are brighter or fainter than the average RGB as indicated in Fig. 10. These stars are marked with open star symbols. The stars marked with filled circles have been used for the metallicity determination. The applied reddening correction is shown as an arrow in the upper left corner.

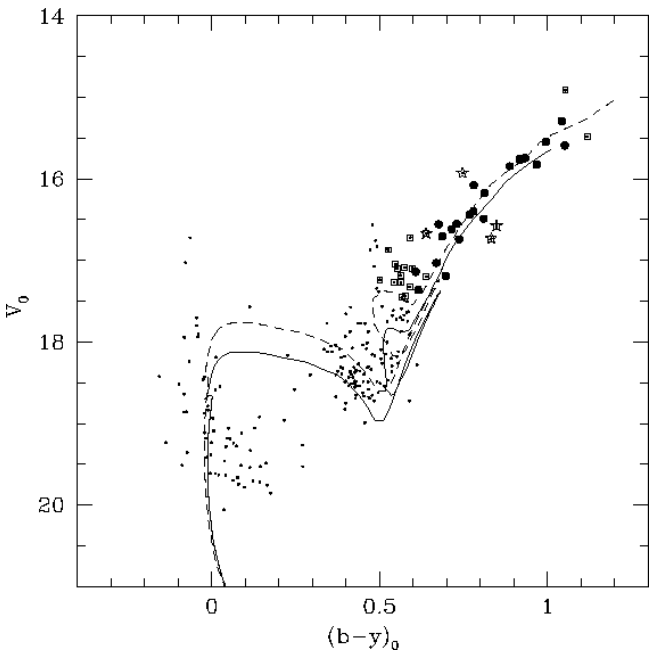

Fig. 10. CMD of the NGC 1806 cluster stars. The overplotted Geneva isochrones have a metallicity of -0.7 dex and ages of $10^{8.7}$ yr (solid line) and $10^{8.6}$ y (dashed line). The symbols are analogous to the ones described in the two-colour diagram for NGC 1806 (Fig. 9).

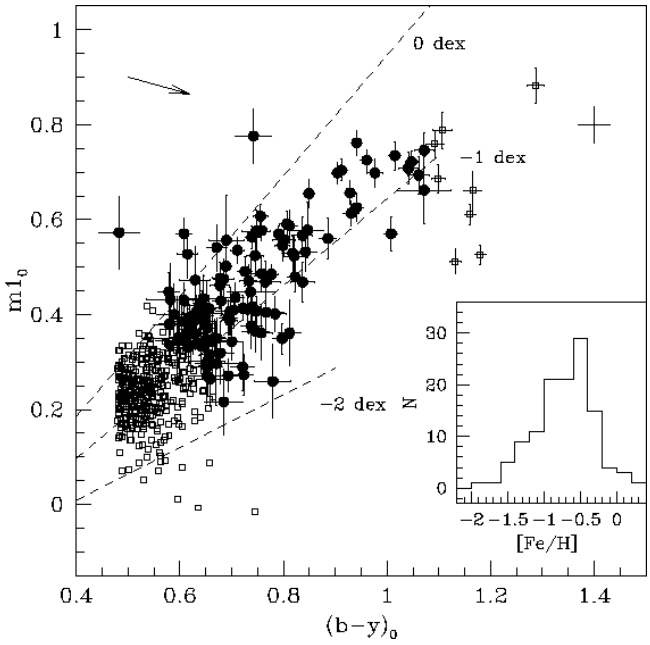

Fig. 11. Field population around NGC 1806 (radial distance larger than $120''$). The filled circles are stars that have been used to determine the mean metallicity of the field and are used for the metallicity histogram shown in the small panel. The open squares on the blue side are stars for which the calibration is valid, but have been excluded according to our colour selection. The open squares on the red side of the two-colour diagram show stars beyond $(b-y)_0 = 1.1$, for which the calibration is not valid any

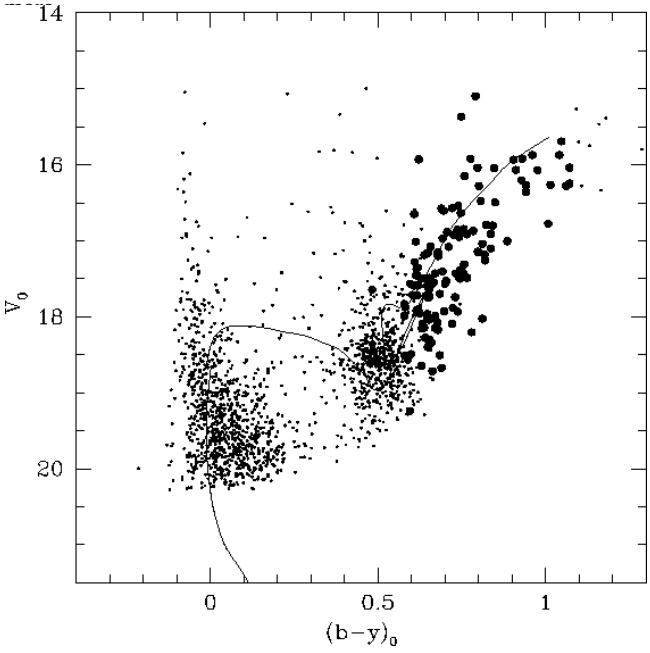

Fig. 12. The CMD of the field stars around NGC 1806. The filled circles are stars which have been used for calculating the mean metallicity. The overplotted isochrone is the same solid one as in Fig. 10 and serves to illustrate the location of the cluster RGB.

The age of this cluster is $10^{8.0\pm0.1}$ yr. In Fig. 14 Geneva isochrones with an age / metallicity of -0.4 dex / $10^{7.9}$ yr and -0.7 dex / $10^{8.1}$ yr are overlayed.

For NGC 2137 we have chosen a radial selection radius of $20''$. Within this radius two stars remain after applying the usual selection criteria. These stars are plotted with stars symbols in the two-colour plot and CMD of NGC 2136/37 (Fig. 13 and Fig. 14). The metallicities and ages of NGC 2136 and NGC 2137 agree well. Therefore, it is plausible that these clusters are a physical pair and not just a chance superposition, as Hilker at al. (1995a) already stated.

9.2. The surrounding field population

The two-colour diagram of the field star population is shown in Fig. 15 and the corresponding CMD in Fig. 16. The stars brighter than $V = 16.2$ are younger than the majority of the RGB stars and are marked with open stars in the two-colour diagram and the CMD of the field population. Unlike the case of the field population around NGC 1711, the younger stars have a lower metallicity than the dominating older RGB field stars, however, also a large fraction of RGB stars have the same metallicity. We measured $[Fe/H] = -0.75$ dex for the mean metallicity and 0.59 dex for the standard deviation. For the younger population (star symbols in Fig. 16) we derive an abundance of $[Fe/H] = -0.46$ and a standard deviation of 0.11 dex. In Fig. 16 an isochrone with a metallicity of -0.4 dex and an age of $10^{8.0}$ yr is plotted that fit these stars.

10. NGC 2031

10.1. The cluster

To select the members of NGC 2031 we chose (from the radial density distribution of stars) $75''$ as a good radius to separate cluster and field stars effectively. In addition to our usual selection criteria we have also excluded the very metal poor star with -2.3 ± 0.3 dex, which is most probably a foreground star, judging from its very deviant metallicity. Another excluded star is slightly above the cluster RGB. However, its metallicity fits well to the metallicity of the cluster. The stars used for the metallicity and age determination are shown in Fig. 17 and Fig. 18.

For this cluster we have found a reddening of $E_{b-y} = 0.06 \pm 0.03$ ($E_{B-V} = 0.09 \pm 0.04$). Mould et al. (1993) quote $E_{B-V} = 0.18 \pm 0.05$ based on HI measurements. Schlegel et al. (1998) give the even larger value of $E_{B-V} = 0.3$ as galactic foreground reddening in this direction. On the other hand derived Schwering & Israel (1991) a reddening of $E_{B-V} = 0.1$. Burstein & Heiles (1982) derived a reddening of $E_{B=V} = 0.07$. Using our reddening value a metallicity of $[Fe/H] = -0.52 \pm 0.21$ can be derived (the error includes the reddening error and the calibration error). With this metallicity we found the best fitting isochrone to be $10^{8.1\pm0.1}$ yr. This agrees well with the age determined by Mould et al. (1993) ($10^{8.14\pm0.05}$ yr with -0.4 dex).

10.2. The surrounding field population

The mean metallicity of the field population for this cluster is $[Fe/H] = -0.75$ dex and the standard deviation 0.44 dex. Definitely young stars are selected in the CMD (Fig. 20) and are marked with open star symbols, while the older stars which can be used to determine a metallicity are marked with filled circles. The metallicity distribution of the older stars is shown in the small panel with the solid line and the distribution of the younger stars with a dashed line. It can be seen, that we do not find young metal poor stars, although we also find older stars with the same metallicity as the younger ones. However, the younger stars are in average more metal rich than the older stars.

11. NGC 1651

11.1. The cluster

The RGB of NGC 1651 merges with the RGB of the field population which can be seen in the CMD of all stars found in the field around NGC 1651 (Fig. A1). This makes the visual separation of field and cluster stars in the CMD impossible. It is only possible to distinguish a few young field stars unambiguously from the mixture of field and cluster RGB.

We decided, after inspecting the radial number density of stars around NGC 1651, to use a radius of $55''$ for the field and cluster separation. In addition we excluded three stars lying well below the cluster RGB. They are most probably foreground stars in the Galactic halo because a LMC star with such a luminosity and metallicity would have an unreasonable age of more than 20 Gyr. Also two stars above the mean RGB of the cluster stars have been excluded. All these excluded stars have been marked in the CMD and two-colour diagram of NGC 1651. The remaining stars used for the metallicity and age determination are shown as filled circles in the two-colour diagram (Fig. 21) and CMD (Fig. 22).

The reddening given by Schwering & Israel (1991) is $E_{B-V} = 0.08$, Mould et al. (1997) used $E_{B-V} = 0.1$ for this cluster, Schlegel et al. (1998) found $E_{B-V} = 0.14$ towards this direction and Burstein & Heiles give $E_{B-V} = 0.1$. With a reddening of $E_{B-V} = 0.1$ the cluster metallicity would be -0.28 ± 0.02 dex. However, no fitting isochrone with such reddening and metallicity can be found. The theoretical RGB stars of this rather large metallicity would be too red or - for younger ages - the main sequence should be visible. The only possibility to fit an isochrone is to use a smaller reddening and hence a lower metallicity. Only with such a metallicity a self-consistent fit in the CMD and the two-colour diagram can be found.

Using $E_{b-y} = 0.03$ ($E_{B-V} = 0.04$) the cluster metallicity derived is $[Fe/H] = -0.58 \pm 0.02$ dex. The two-colour diagram for this reddening is shown in Fig. 21. The calibration error accounts for an additional error of 0.19 dex. Using this metallicity the age is $10^{9.3\pm0.1}$ yr. The isochrone is overlayed to the cluster CMD in Fig. 22.

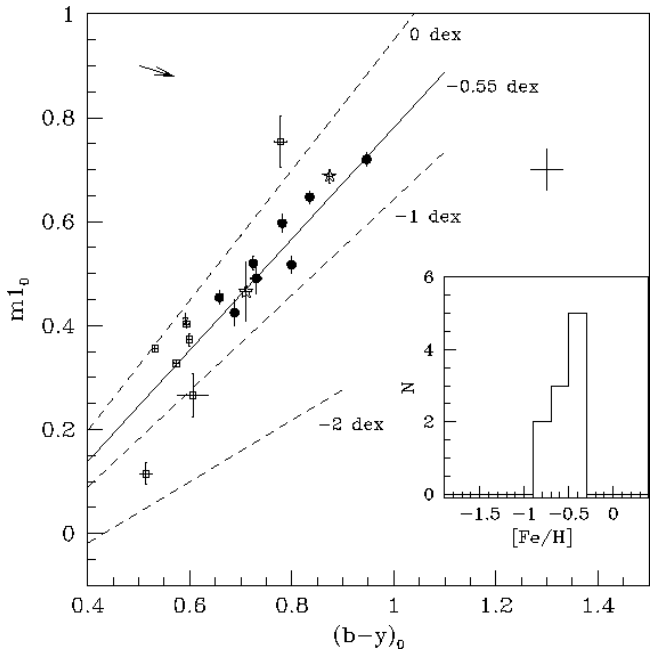

Fig. 13. Two-colour diagram of NGC 2136/37. Solid dots are used for stars which have been used to determine the metallicity of NGC 2136. The two open star symbols show the giants that belong to NGC 2137. Open squares bluer $b-y=0.6$ mark stars for which the calibration holds, but which have been excluded. The apparently metal rich stars has been excluded because of its deviant location from the other giants in this diagram. The histogram shows the metallicity distribution of the NGC 2137 and NGC 2136 giants.

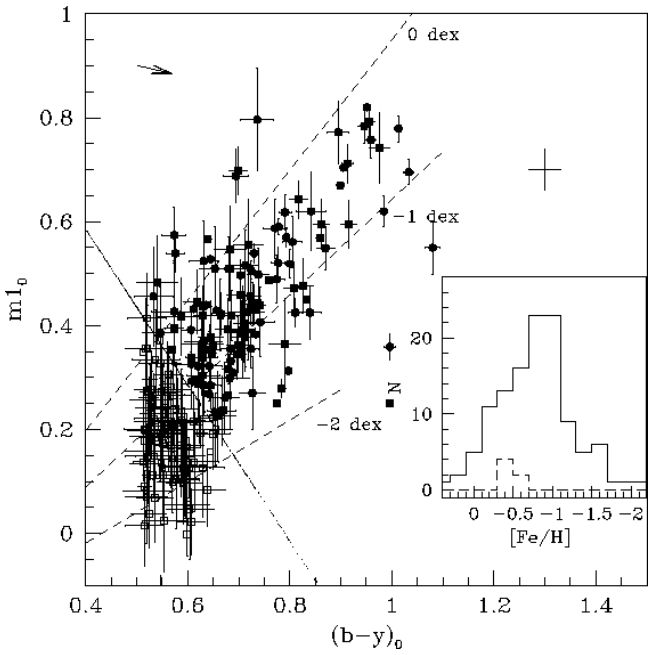

Fig. 15. Two-colour diagram for the field stars around NGC 2136/37 (further than $120''$ away from the centre of NGC 2136 and further than $50''$ away from the centre of NGC 2137). Filled circles and open stars symbols mark stars that have been used to calculate the mean and standard deviation of the field star metallicity. Open squares show stars for which the calibration is in principle valid, but they have been excluded due to our colour selection. In the insert the solid line shows the metallicity distribution of all stars redder than the colour selection line, the dashed line indicates the metallicity distribution of the younger stars which are indicated by the open star symbols in the CMD ((Fig. 16).

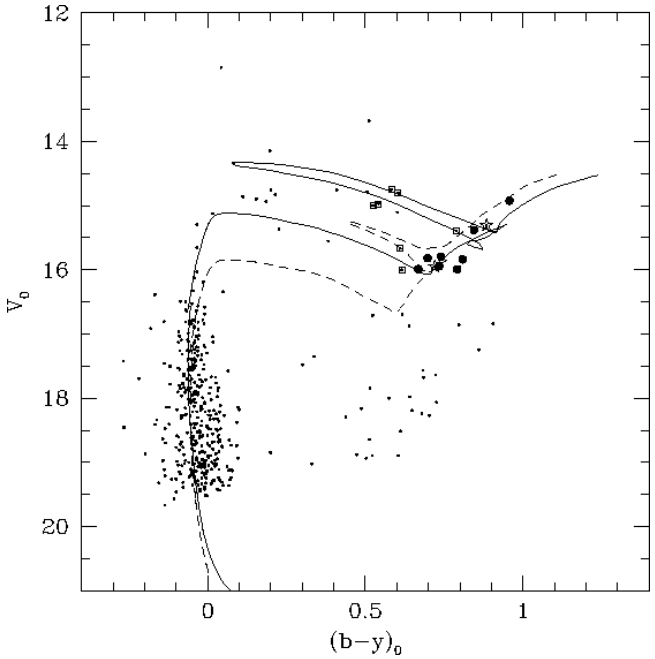

Fig. 14. CMD of the NGC 2136/37 stars. The red giants used for the metallicity determination are denoted by the same symbols as in the two-colour diagram (Fig. 13). Overlayed is a -0.4 dex Geneva isochrone with an age of $10^{7.9}$ yr (solid line) and one with a metallicity of -0.7 dex and an age of $10^{8.0}$ y (dashed line).

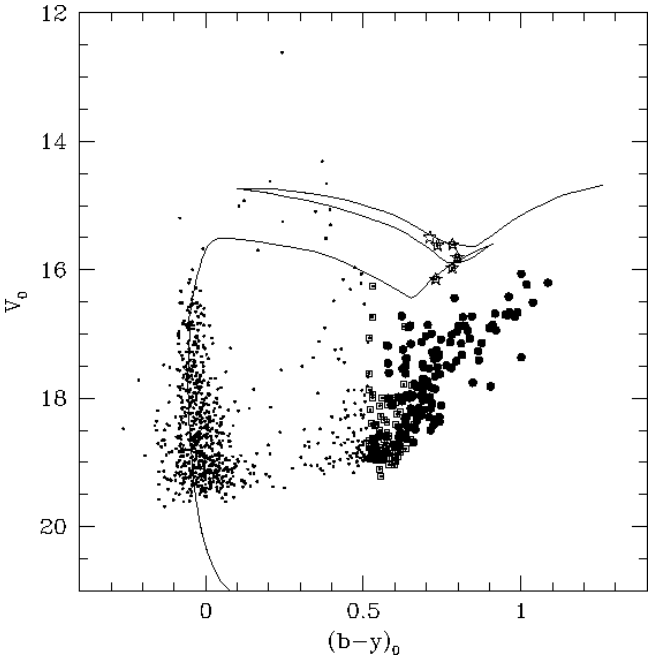

Fig. 16. CMDs of the field population around NGC 2136/37. The symbols of the marked stars are the same as the two-colour diagram (Fig. 15). The isochrone has an age of $10^{8.0}$ yr and a metallicity of -0.4 dex.

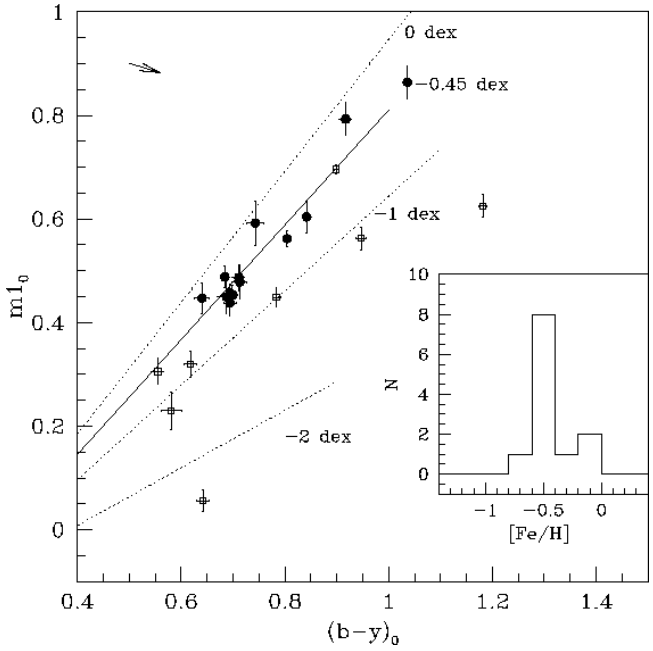

Fig. 17. Two-colour diagram of the stars within $80''$ from the centre of NGC 2031. The stars that have been used for the determination of the metallicity of NGC 2031 are shown with solid circles and in the insert with the solid line in the histogram. Excluded stars are displayed using with open squares: one is redder than the used colour range, four are bluer and 2 stars lie well apart from the mean location of the other stars in the CMD shown in Fig. 18.

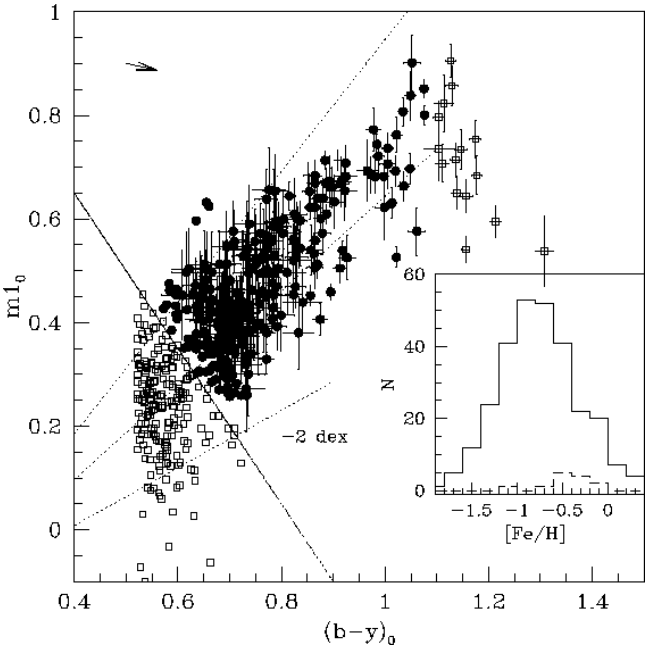

Fig. 19. Two-colour plot for the field stars around NGC 2031 (with a radial distance larger than $110''$). Filled circles mark stars which have been used to calculate the mean and standard deviation of the field star metallicity. The open squares indicate excluded stars In the small panel the solid line shows the metallicity distribution of the older stars, the one of the younger stars is plotted using a dashed line. The younger stars are selected in the CMD (Fig. 20) and are marked in the CMD with open star symbols.

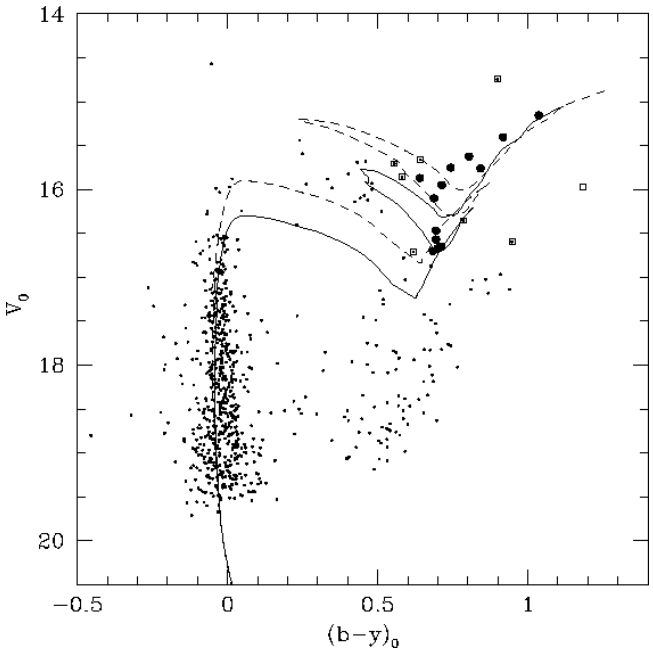

Fig. 18. CMD of NGC 2031. The symbols are the same as those in Fig. 17. Overlaid are Geneva isochrones with a metallicity of -0.4 dex and an age of $10^{8.0}$ yr and $10^{8.1}$ yr, respectively.

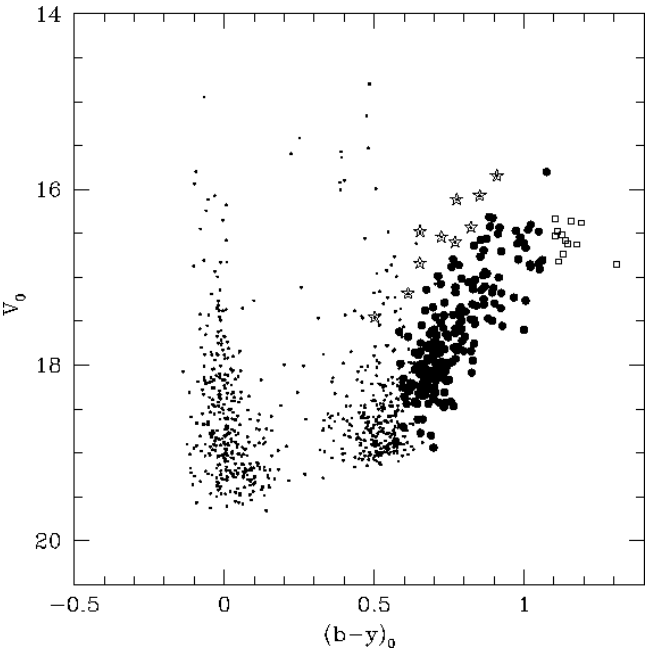

Fig. 20. CMD of the field population surrounding NGC 2031 (they have a distance of more than $110''$ from the cluster centre). The filled circles are the older stars that have been used for the metallicity determination of the field. The open star symbols have been selected due to their younger age, their metallicity distribution is shown in the insert in Fig. 18 with the dashed line.

However, this solution is not unique: also with a smaller reddening acceptable fits are possible, resulting in larger ages and smaller metallicities, hence we only got a range of parameters for this cluster: $0.01 < E_{b-y} < 0.05$, $-0.65 < [Fe/H] < -0.45$, $10^{9.4} > lg(Age) > 10^{9.0}$. The calibration uncertainty has to be included into these upper and lower limits. Three stars around this cluster have been spectroscopically investigated by Olszewski et al. (1991). Two have been identified, both being very red ($(b-y) > 1.3$. They are also identified AGB stars (Frogel & Blanco 1990). These stars have a metallicity of -1.33 dex and -1.6 dex, a more metal rich (-0.37 dex) AGB star could not be identified.

NGC 1651 has been observed with the HST by Mould et al. (1997). They derived an age of $10^{9.2\pm0.1}$ yr (using $[Fe/H] = -0.4$ dex). The age is in good agreement despite the metallicity discrepancy.

The elongated and tilted red clump of the cluster (see Fig. 22) is a feature that remains worth mentioning. The elongation is approximately along a reddening vector, however strong differential reddening should not cause this shape since the RGB does not show a similar large colour spread. We consider it more probable that this it is an intrinsic feature of an HB of a certain age and metallicity. The red clump of the field population does not show this elongated shape, it is rather a slightly fainter clump. Such an elongated red clump has also been observed by Piatti et al. (1999) with in the Washington system in three of their 21 investigated fields. In case of NGC 2209 they discuss the possibility that an increased helium content or differential reddening could cause such a red clump morphology.

11.2. The surrounding field population

The dominating field population around NGC 1651 $[Fe/H] = -0.75$ using the low reddening of $E_{b-y} = 0.04$. The two-colour diagram for the field population is shown in Fig. 23 and the corresponding CMD in Fig. 24. The red clump of the field population is not elongated and slightly fainter.

In this field, two groups of stars show up with distinct metallicities: one group with an approximately solar abundance ($[Fe/H] = 0.03 \pm 0.03$ dex) and one group around -1 dex. The metal poor stars can be fitted with a Geneva isochrone of -1 dex and an age on the order of $10^{9.6}$ yr. However, it is impossible to find a fitting isochrone for the apparent more metal rich stars (around 0 dex), since these stars would have an age around $10^{8.5}$ yr and thus many more main sequence stars should be present. Only with the assumption of no reddening being present, one would have derived a metallicity of $[Fe/H] = -0.21 \pm 0.19$ dex for these stars. With such a metallicity they could have been fitted with a $10^{8.8\pm0.1}$ yr Geneva isochrone.

12. NGC 2257

12.1. The cluster

The oldest cluster in our sample is NGC 2257, which can be seen from the cluster CMD (Fig. 26) that is very similar to the CMDs of Galactic globular clusters. Especially the pronounced blue horizontal branch (HB) is a sign for an old, metal poor population. NGC 2257 lies $\simeq 9^0$ away from the centre of the LMC to the north east. Because of this large distance the field is very sparsely populated, thus we renounced a radial selection, because no radius can be found at which the field stars dominate.

No reddening determination via a main sequence is possible. However, only a reddening of less than $E_{b-y} = 0.06$ results in consistency of a reasonable age with a reasonable metallicity. We adopt here the reddening used by Testa et al. (1995), $E_{B-V} = 0.04$ and an error of $\Delta E_{B-V} = 0.04$. Schwering & Israel's map (1991) shows a reddening of $E_{B-V} = 0.03$ at position of NGC 2257, Schlegel et al. 1998) give $E_{B-V} = 0.06$ and Burstein & Heiles (1982) $E_{B-V} = 0.04$. With a reddening of $E_{B-V} = 0.04$ the metallicity measurement results in $[Fe/H] = -1.63 \pm 0.21$ dex (including the calibration errors). In the two-colour diagram the metallicity determination is illustrated in Fig. 25.

The age has been determined like in the previous cases, however since no Geneva isochrone with such an age and metallicity had been available we used Padua isochrones. The best matching (-1.7 dex) isochrone is overlaid on the CMD of this field in Fig. 26. The RGB of an old population evolves slowly and thus its location does not differ much between different ages. Therefore, we can only define an age range from 10^{10} yr to $10^{10.3}$ yr for this cluster, when limiting the age determination to the RGB. If the isochrones represent well the colour of the HB, then the age uncertainty will drop severely, since the HB of younger clusters is much redder (around $(b-y) \simeq 0.3$) than that of older ones. In this case the allowed age range is merely $10^{10.24} - 10^{10.30}$ yr. The linear age uncertainty is much larger than for the younger clusters, discussed above. The reason for this is not an increased photometric error, but rather an intrinsic effect of the age-luminosity evolution: the brightness (in magnitudes) of the RGB decreases with age approximately logarithmically, therefore the error in the age of young and old stars should be in first order the same in the *exponent*. For the younger cluster this error was around 0.1, comparable to the error in case of NGC 2257.

Testa et al. (1995) obtained deep B and V HST observations and concluded from the Turn-Off location and an assumed metallicity of -1.7 dex that the age is $\simeq 10^{10.1}$ yr. Geisler et al. (1997) found an age of $10^{10.07}$ yr. Recently, Johnson et al. (1999) used deep HST observations of three true LMC globular clusters including NGC 2257 to derive their relative ages compared to Galactic globulars. They found that these old clusters have an age that is not distinguishable from that of M 3 and M 92.

12.2. The surrounding field population

In spite of the low stellar density, a few field stars could have been identified due to their deviating age and metallicity. In the two-colour diagram (Fig. 25) stars having a metallicity around -1 dex and being redder than $b-y = 0.6$ have been marked

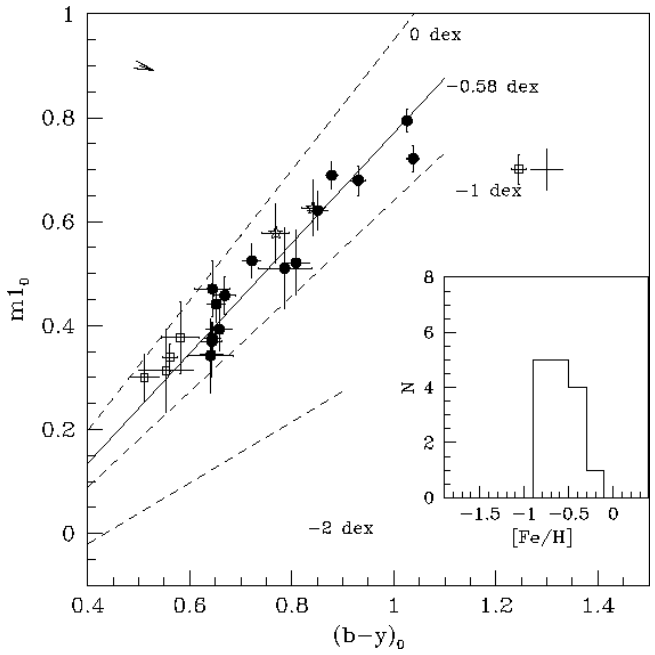

Fig. 21. Two-colour diagram of NGC 1651. The cluster stars have a distance of less than $60''$ from the cluster centre. The filled circles denote stars which have been used for the metallicity determination. The stars marked with open star symbols have been excluded because they deviate considerably from the mean RGB location in the CMD of this cluster (Fig. 22).

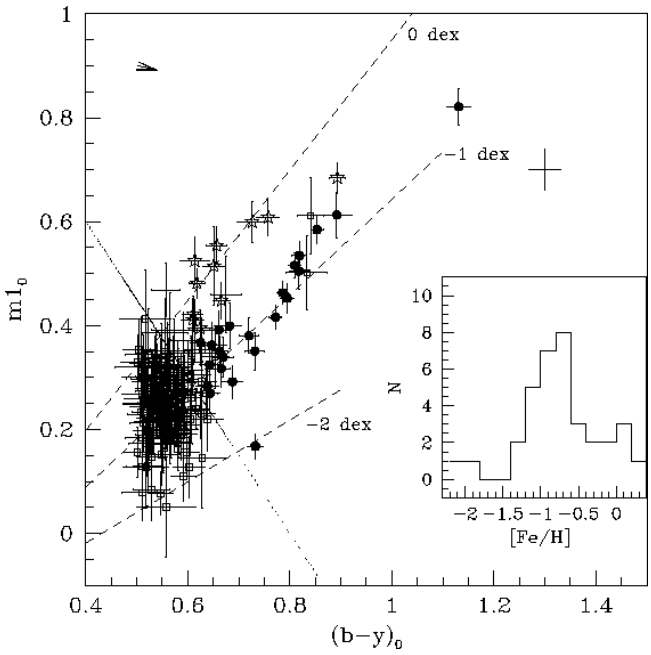

Fig. 23. Two-colour diagram of the field population around NGC 1651. The stars that have been used for the metallicity determination are marked with filled circles and open star symbols. In the insert their metallicity distribution is plotted as histogram. The separation into stars marked by filled circles or open star symbols has been applied according to their location in the two-colour diagram (metal poor/ metal rich).

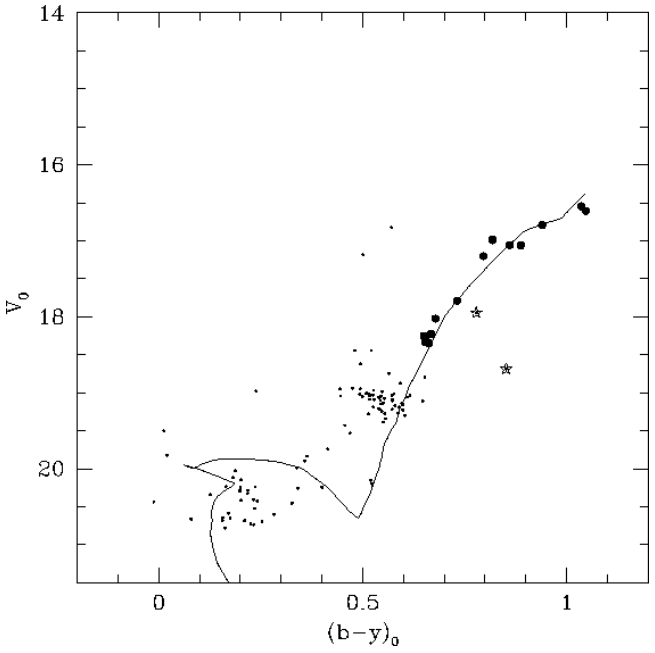

Fig. 22. CMD of NGC 1651 with a -0.4 dex, $10^{9.1}$ yr (solid line) isochrone and a -0.7 dex, $10^{9.2}$ yr isochrone over-plotted. The filled circles are the stars that have been used for the metallicity measurement.

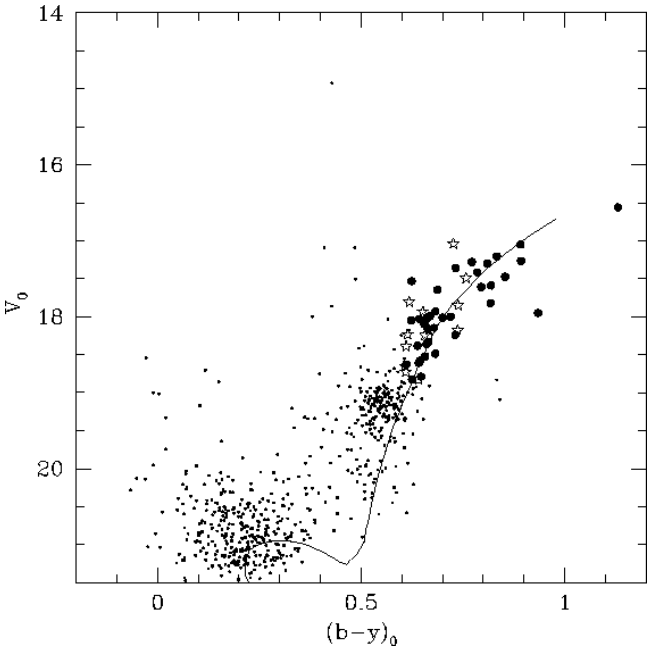

Fig. 24. CMD of the field population around NGC 1651. The symbols correspond to those used in Fig. 23. The isochrone has a metallicity of -1 dex and an age of 4 Gyr.

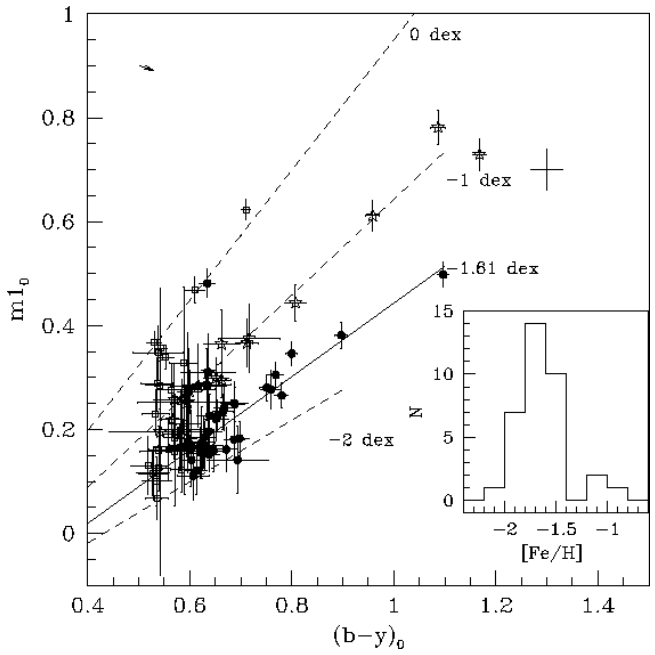

Fig. 25. Two-colour diagram of the stars in the field of NGC 2257. Since no radial selection criterion has been applied, stars have only been selected in the CMD, according to colour and luminosity. Stars being most probable cluster members are shown as filled circles, stars fainter the mean RGB are shown as open star symbols and brighter stars as squares. Stars bluer $(b-y) = 0.6$ for which the calibration is valid, but have been discarded are shown as open squares as well. For the selection criterion also refer to Fig. 26.

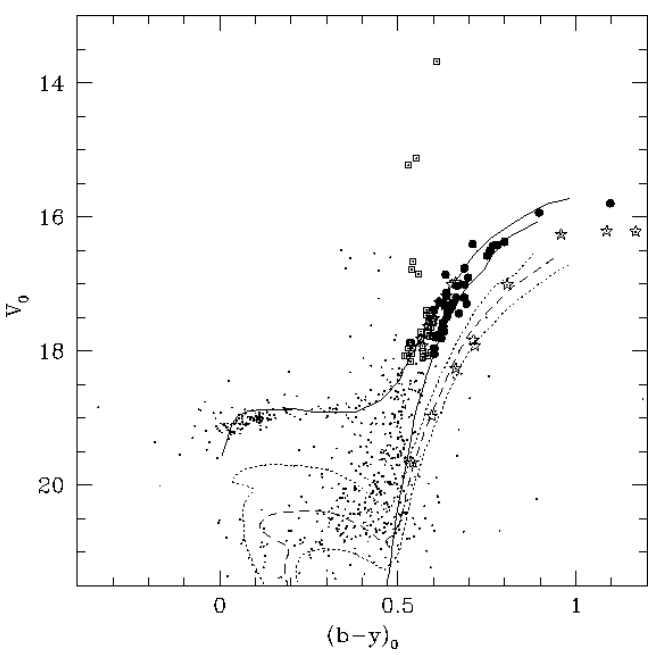

Fig. 26. CMD of the stars around NGC 2257. The solid Padua isochrone has a metallicity of -1.7 dex and an age of $10^{10.24}$ yr. The dashed Geneva isochrone has a metallicity of -1 dex and an age of $10^{9.4}$ yr and the dotted Padua isochrones have -1.3 dex and $10^{9.2}$ yr, $10^{9.6}$ yr. Symbols as in Fig. 25.

with open star symbols. These stars form in the CMD (Fig. 26) a RGB lying below the cluster RGB. With a metallicity of $[Fe/H] = -1$ dex the age of the population is $10^{9.4}$ yr. No other field component (except probably some Galactic foreground stars around $(b-y) = 0.5$) have been found.

The age and metallicity obtained for the field stars agrees well with the values found for the field population around the investigated clusters that are closer to the LMC centre. This indicates that, if a radial metallicity gradient exists, it cannot be very pronounced. This is consistent with the result of Olszewski et al. 1991 who did not find a radial metallicity gradient in the cluster population of the same age. However, there is a metallicity gradient in the sense that younger clusters and field stars tend to be more concentrated (Santos Jr. et al. 1999) and thus the mean metallicity of all stars should show a metallicity gradient. In contrast Kontizias et al. 1993 found a metallicity gradient in the outer cluster system while none was observable for the inner clusters.

The field population in the vicinity of NGC 2257 has been studied by Stryker (1984). Her analysis revealed that the metallicity of the field population is larger than that of NGC 2257 and that *"star formation occurred in the field long after the formation of the cluster"*. She estimated the age of the field component to be $6-7$ Gyr old. We recalculated the age of this population based on her photographic CMD: we estimated the luminosity difference between the turn-off of this population and its red HB to be $\Delta V = 2 \pm 0.3$. Walker et al. (1993) also found a younger field population around NGC 2257 with HST observations. The field population around this cluster is best fitted by a Padua isochrone with an age of 3.5 gyr and a metallicity of -0.6 dex. Using $[Fe/H] = -1$ and applying the calibration given in Binney & Merrifield (1998) we end up with an age of 4 ± 1 Gyr for this population which is comparable to our derived age.

13. The method to derive an AMR and SFH of the field population

In order to extract detailed information concerning an AMR and/or the chemical enrichment history of the field, it is necessary to use a more sophisticated analysis than just deriving a mean metallicity and its standard deviation. Thus we estimated an age for each star with a measured metallicity. For these measurements a set of isochrones with different ages for each metallicity has to be available. Therefore we interpolated Geneva isochrones linearly to generate isochrones that are continuously distributed in metallicity. For each star the isochrone of the appropriate abundance with the minimal luminosity difference to the star has been identified and the corresponding age has been assigned to the star. This method obviously resulted in discrete age binning for the field stars (the size of the age bins is $log(t) = 0.1$). We did not interpolate in age, since the age uncertainty due to the discrete age sampling is smaller

than the error due to the photometric error, the calibration error and the errors connected to reddening and blending.

Our method is not free from ambiguity, since for most stars one can derive two solutions, one for the RGB and one for the AGB. For stars older than $10^{9.3}$ yr one can neglect this effect because **a)** the luminosity difference between the AGB and RGB and thus the inferred age difference is small compared to the other uncertainties in determining an age for these evolved stars and **b)** the fraction of AGB to RGB stars in our colour range is small due to the lifetime difference. For younger ages the AGB stars play a considerable role: they dominate in the used colour range for populations with an age between $10^{8.5}$ yr and $10^{9.1}$ yr (see e.g. the overlayed isochrone in Fig. 10). To account for this problem we used the following approach: we determined an AGB age and a RGB age for each star. If the AGB *and* the RGB age were older than $10^{9.3}$ yr we assigned only a RGB age to the star. In case that we found a RGB age between $10^{8.4}$ yr and $10^{8.7}$ yr we used the AGB age to account for the dominance of the AGB stars in our used colour range. For the other ages we used either a mean AGB & RGB age, if none of the isochrones had a luminosity difference of less than 0.1 mag or we used the age that correspond to the isochrone with a luminosity difference of less than 0.1 mag to the star.

The uncertainties in the extension of the isochrone towards the red is not critical for this investigation as long as one is not concerned with the number of stars with a certain age/metallicity. More severe are possible problems in the shape of the theoretical models, which might result in a systematic shift or distortion in the age scale, thus all our results on the field population is valid for the only currently available Strömgren isochrone set. However, since these isochrones fit reasonably well to the studied clusters, we are confident that the AMR is quite robust concerning the applied isochrones. We cannot circumvent this problem and it is necessary to get Strömgren isochrones for more recent stellar models with which the results can be compared.

Since the age resolution on the RGB is not very good the derived age for an individual star is not more precise than a factor of 2 for older stars, therefore all results can only be interpreted statistically.

The applied procedure resulted in an AMR and an age number distribution (AND). The latter can be used to derive the Star Formation History (SFH) of the combined population. However, one has to bear in mind that the AND is not just the star formation rate (SFR) counted in logarithmic bins. First and most obvious is the fact, that stars of different ages have different masses on the RGB. Therefore one has to account for the IMF to get the SFH. Secondly, systematic shifts, for example due to differential reddening or binaries, have to be considered. Finally one has to be aware of the fact that the conclusions depend sensitively on the used set of isochrones. Taking all these effects into account is a highly complex problem and there is little hope to disentangle them analytically. To get nevertheless a handle on these effects and an idea about the accuracy of our method, we created synthetic CMDs of field populations with different ages and metallicities using a Monte Carlo algorithm and Geneva isochrones. The program allows one to include the (measured) errors, differential reddening, depth structure, a binary fraction and arbitrary SFHs. Binaries have been chosen randomly (according to a white random distribution) and are not important for the further investigation that regards only red giants. Even apart from the problems in interpreting the AND, the age distribution and thus the SFH depends rather strongly on the assumed reddening and possible differential reddening. Thus the results should be regarded more in comparison with the SFH derived with deep photometry (e.g. Gallagher et al. 1996, than as an independent measurement of the starformation history. Holtzman et al. 1999, Elson et al. 1997, Romaniello et al. 1999) and serve as a consistency check.

13.1. Tests with simulated data

To test our applied method we generated several artificial data sets. In Fig. 27**a,b** we show the resulting AMR and AND of two of these simulations. The left one (**a**) consists of three populations with $10^{8.4}$ yr, -0.2 dex and $10^{9.1}$ yr, -0.4 dex and $10^{9.8}$ yr, -0.7 dex, respectively. The number ratio old-to-young-stars is $1:1:10$. No error was applied. In the right two panels (Fig. 27**b**) we have included the photometric errors, a binary fraction of 70% and differential reddening of $\Delta E_{B-V} = 0.04$. The IMF used in both simulations (a Salpeter IMF down to $0.8 M_{\odot}$) is not important for the resulting AMR because of the small mass interval on the RGB. The open circles show the input age and metallicity, while filled circles are used for the extracted mean values for the metallicity. However, the IMF is an essential input parameter when deriving a SFH. Fortunately, it is not very critical for relative number ratios as long as the IMF did not change with time. This is an ad hoc assumption in our simulation since we cannot constrain any mass function with our method. The AMR of the input population in the shown simulation follow the AMR proposed by Pagel & Tautvaišvienė (1998). Thus this simulation demonstrates our ability to be able to recover the shape of the AMR proposed by these authors (on the basis of the given isochrones). It is impossible to see potential bursts in the SFH and it is clear that it is very difficult to derive the SFH from this procedure, only rough estimations of the SFH can be made.

13.2. Tests with the observed fields

We tested our method also with the aid of the observed cluster stars. We used radially selected samples around the cluster centre and determined for them automatically the mean age and metallicity. The results are shown in Table 3 where also the error of the mean metallicity and the standard deviation (σ([Fe/H]) and σ(log(Age [y]))) is given for each cluster. The results for all clusters (except for NGC 2257, see below) are in good agreement with the ages that had been found with isochrone "fitting". For NGC 2257 we did not expect to find the cluster's age and metallicity since or method applies only to stars having an age of less than ≈ 10 Gyr and a metallicity of more than -1.5 dex. The standard deviations around the

Table 3. Automatically determined age and metallicity of the investigated clusters

Cluster	[Fe/H]	σ([Fe/H])	log(Age [y])	σ(log(Age [y]))
NGC 1651[1]	-0.63 ± 0.04	0.26	9.24 ± 0.06	0.35
NGC 1806	-0.56 ± 0.04	0.32	8.66 ± 0.05	0.38
NGC 2031	-0.45 ± 0.05	0.19	8.16 ± 0.07	0.26
NGC 2136/37	-0.56 ± 0.03	0.10	8.16 ± 0.05	0.16
NGC 2257[2]	-0.85 ± 0.10	0.29	9.27 ± 0.14	0.40

[1] A reddening of $E_{b-y} = 0.03$ has been used. [2] The whole field of NGC 2257 is used.

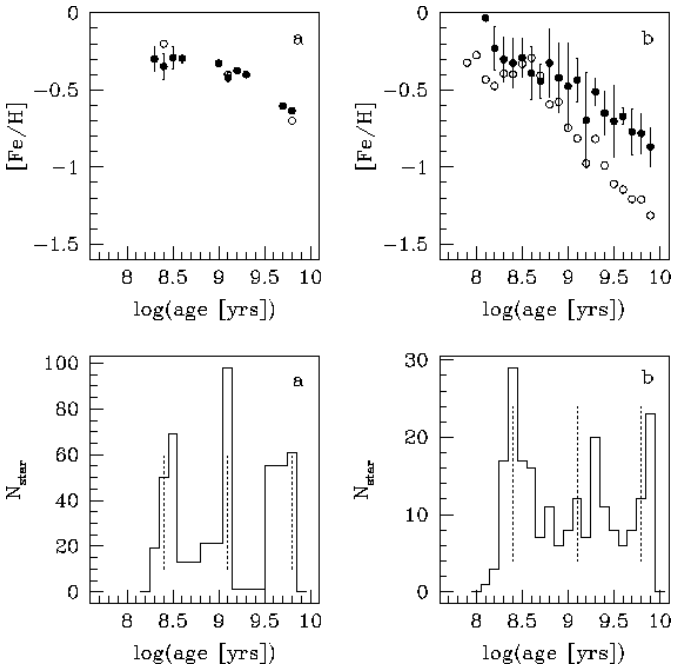

Fig. 27. The age-metallicity relation (AMR) and the age-number diagram (AND) of two simulations are shown to demonstrate the effect of selection effects, photometric errors and systematic uncertainties. The input of the simulation consists of three discrete populations with $10^{8.4}$ yr, -0.2 dex, $10^{9.1}$ yr, -0.4 dex and $10^{9.8}$ yr, -0.7 dex as age and metallicity, respectively. The number ratio is $1 : 1 : 10$. In the left panel **a** no error was applied, in the right panel **b** we assumed the same photometric errors as for NGC 1711, a binary fraction of 70% and a differential reddening of $\Delta E_{B-V} = 0.04$ (peak to peak). The open circle indicate in **a** the input population's age and metallicity and in **b** our measured mean AMR. Filled circles are used for the mean metallicity we derived from the simulated measurements. The dotted lines in the lower graphs illustrate the input population's age.

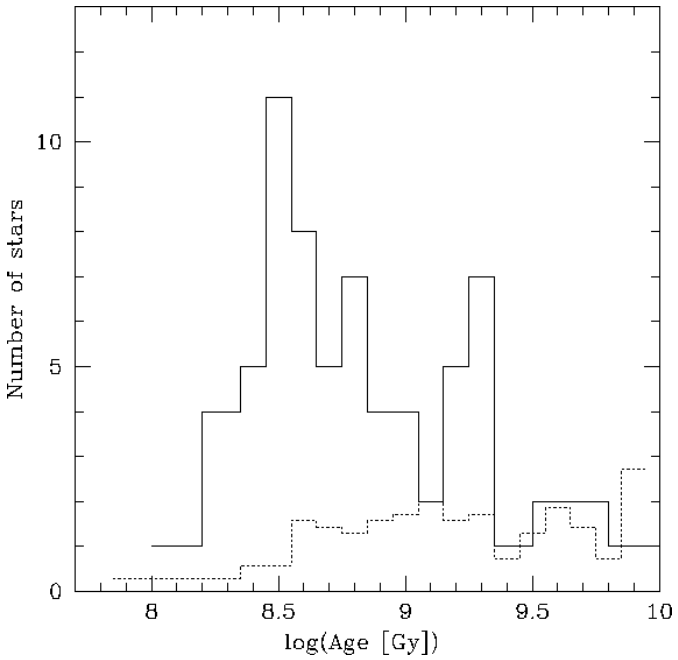

Fig. 28. The age distribution of stars around the combined fields of NGC 1806 and NGC 1651. The solid lines shows the number of stars recovered when stars are used that are less than $75''$ away from the centre of NGC 1651 and 60" from the centre of NGC 1806. We used a smaller selection radius for NGC 1806 since this cluster appears considerably larger than NGC 1651 and we wanted to get comparable results. Stars nearer than $20''$ to the cluster centre have been excluded. The dotted line are the number of field stars around these clusters scaled to the same area.

mean values are considerable, however, systematically $\approx 25\%$ smaller than for the field populations.

In Fig. 28 we show for two clusters one with a pronounced RGB and the other with a AGB the result of this method. We use the stars up to a distance of $60''$ and $75''$ around NGC 1806 and NGC 1651, respectively, as a combined input. The clusters can be seen as peaks at the corresponding age ($10^{9.2}$ yr, $10^{8.7}$ yr). The selection radius for NGC 1651 was two times larger than the one we used to derive the cluster's age and metallicity via isochrone fitting. In Fig. 28 the age distribution of the field stars scaled to the same area as the cluster stars is plotted with the dotted line.

14. The AMR of the combined field population

A major problem in deriving a reliable AMR and SFH is the small number statistic of field stars available for such an investigation after applying the selection criteria. To overcome the statistical problems, we have summed up all the CCD fields to work on a "global" LMC field population. With this approach, we are able to present an overall picture of the field AMR of the observed regions. Our sample of field stars (comprising 693 RGB stars, for which an age and a metallicity has been mea-

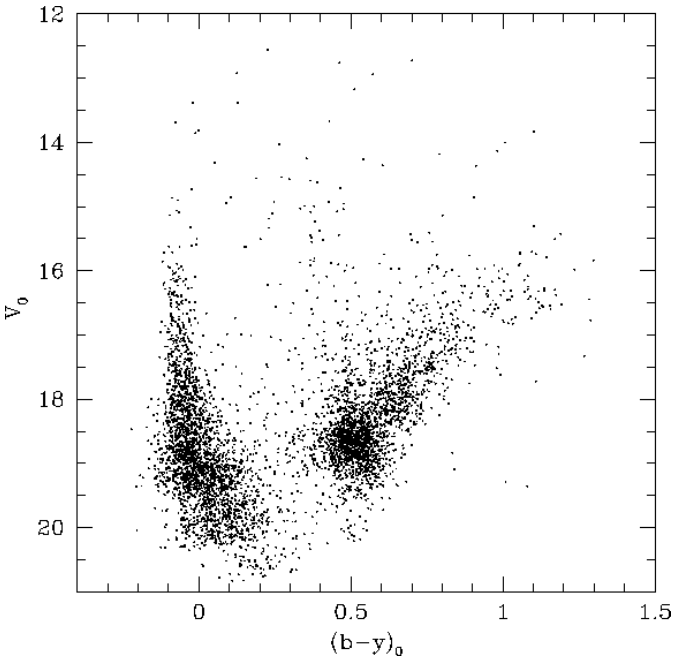

Fig. 29. CMD of all field stars found around the investigated clusters. Only stars are plotted that fulfil the error selection criteria (see Sect.4.2).

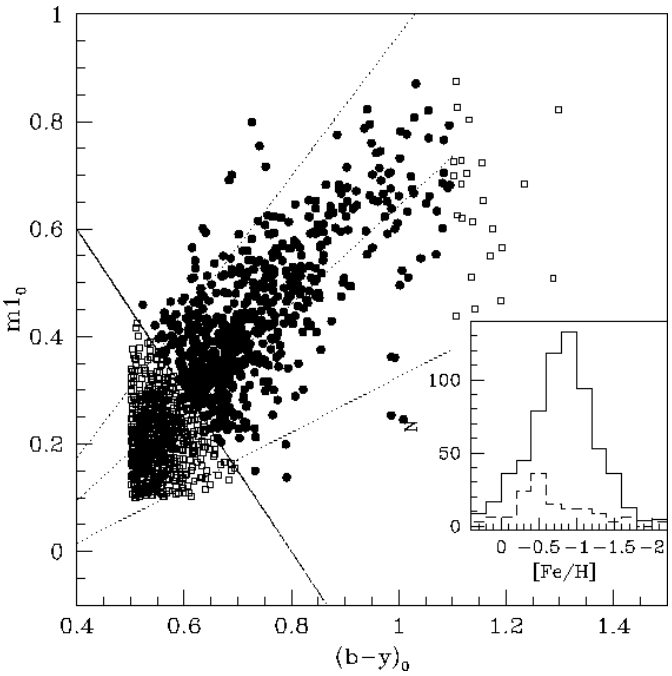

Fig. 30. Two-colour diagram of all field stars found around the investigated clusters. Solid circles are used to mark stars with a reliable metallicity measurement. Stars being redder than $(b-y)=1.1$ have been excluded, as usual. The solid histogram in the insert shows the metallicity distribution of all stars, the dashed line the distribution of stars being younger than $10^{8.4}$ yr.

sured) enabled us to derive a "global" AMR and AND, where "global" rather means an average over our pointings. The distances of our inner clusters from the LMC centre are between 1.6^0 and 4^0. This corresponds to a projected distance difference of approximately 2 kpc between the investigated fields. However, we did not weight these different fields and thus our results are more influenced by the stellar population around NGC 2031 and NGC 1806 than by for example the field stars around NGC 1651. Since after 1 Gyr the stars should be well mixed within the LMC (Gallagher et al. 1996; they assumed 1 km/sec as velocity dispersion of a typical LMC star). Thus this sample has a global meaning at least for the stars being older than 1 Gyr.

The CMD and two-colour diagram of this combined population is shown in Fig. 30 and Fig. 29, respectively.

The derived AMR is shown in Fig. 31 and tabulated in TableA3. The plotted "error" bars give the standard deviation in metallicity of stars with the same age and is not an error of the mean metallicity, since we do not believe that in each age bin all stars have the same metallicity even if we could measure the age with much higher accuracy. The age resolution on the giant branch drops considerably for stars that are older than $10^{9.2}$ yr because the spacing in luminosity between isochrones of different ages shrinks. This could cause the flat appearance of the AMR for these old ages, which is compatible with the shown "error" bars.

The upper age limit of our investigation is $10^{9.9}$ yr because no older Geneva isochrones were available, the lowest metallicity of the Geneva isochrone set is -1.3 dex. For stars that are more metal poor we used the -1.3 dex isochrones to derive the age (if the luminosity difference between the star and the isochrone was < 0.1 mag), which means an underestimation. With these stars included, the oldest bin of the AMR contains stars, which in reality are older and more metal poor than the above stated limits. Therefore the number of stars in the age range $10^{9.5}$ yr - $10^{9.9}$ yr is slightly overestimated.

The colour selection can introduce a bias, since the RGB of a metal rich population lies completely in the employed colour range, while for example only half of a -1.3 dex RGB extends so far red which can be seen from the employed isochrones. The fraction of the RGB within the selected colour range is in good approximation independent of the age as long as stars older than 1 Gyr are considered (concluded from visual inspection of the employed Geneva isochrones). For younger ages the problem becomes less severe, since the red supergiants extend further red. Since all our conclusions on the metallicity are based on simple means this introduces a bias towards higher metallicities if equal aged stars with different metallicity exist. To estimate the amount of the most extreme shift, we assume two populations with the same age but one having solar abundance and the other having a metallicity of -1.3 dex. The difference in the mean metallicity, if only half of the metal poor giants are observed compared to the mean metallicity of the whole sample is $\Delta[Fe/H]_{mean} = -1.3(1/2 - 1/3) = 0.2$ dex. Thus we conclude that deviations due to this problem are well less than 0.2 dex.

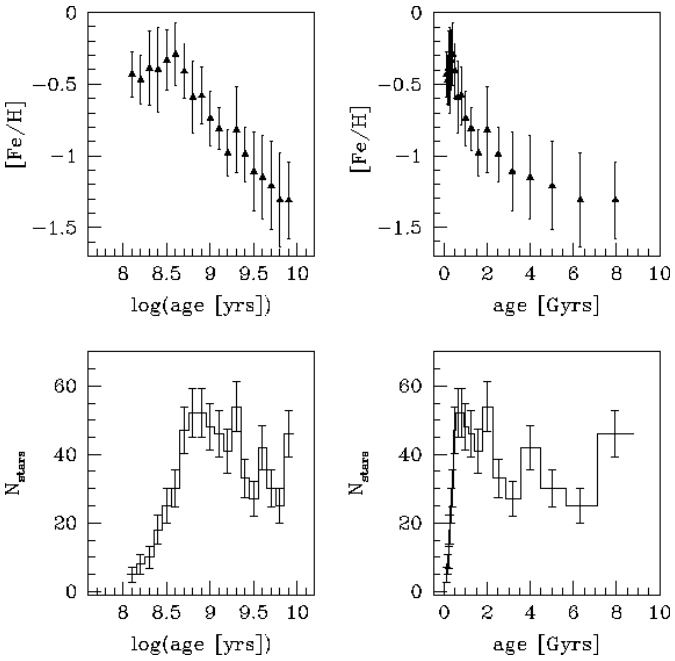

Fig. 31. The AMR and AND in logarithmic and linear age representation of all field stars around the investigated cluster.

The CN anomaly leads to an overestimation of the metallicity and hence to an underestimation of the age. The deviation of the age according to the deviation of an overestimation of the photometric metallicity is nearly parallel to the observed AMR for ages larger than $10^{8.5}$ yr. Even with CN anomalous stars we should be able to distinguish between the proposed AMR and for example the AMR propposed by Pagel & Tautvaišviennė (1998): the influence of CN anomalous stars on the second AMR would result in an even more pronounced difference as it is already seen, since metal poorer stars would be shifted to even more metal rich and younger locations.

15. Discussion

15.1. The Age-Metallicity Relation

In Table4 we summarise the resulting ages and metallicities of the investigated clusters.

In order to compare our results with the literature, we compiled a list of clusters with ages and metallicities according to various sources (all published after 1989). The data is tabulated in TableA5. In addition, we used the compilation of Sagar & Pandey (1989), from which only clusters have been selected with a limiting magnitude below $V = 21$. This limit shall serve as a rough quality criterion that is comparable to the more recent data and explains why most (photographic) papers cited by Sagar & Pandey are excluded. These clusters are plotted together with the newly investigated clusters and our field AMR in Fig. 32. The solid line is the field AMR accompanied by two dotted lines which mark 1σ borders. If the older clusters are excluded, a weak correlation appears for the clusters: clusters younger 1 Gyr have a mean metallicity of $[Fe/H] = -0.34$ with a standard deviation of 0.14 and in the age range $1 - 2.5$ Gyr the mean metallicity is $[Fe/H] = -0.71$ with a standard deviation of 0.17 (11 cluster).

The mean metallicity of our young clusters ($< 10^{9.0}$ yr) is -0.57 ± 0.04 dex and thus lower than what we found using the newer cluster sample from the literature. The field of the same age has a mean metallicity of -0.4 ± 0.2 dex and is in good agreement with spectroscopic measurements (-0.38 ± 0.11 dex) of young field stars. The latter comparison is reasonable since **a)** most of the stars for which high resolution spectroscopy has been obtained are located at a similar radial distance and **b)** no radial gradient can be seen in the spectroscopic sample. We compiled a list of high resolution spectroscopic measurements of LMC stars in Table A4.

Bica et al. (1998) obtained ages and metallicities of 13 outer clusters in the LMC using Washington photometry. The mean metallicity of all the surrounding field stars is $\langle [Fe/H] \rangle \simeq -0.6 \pm 0.1$. The mean metallicities of our field populations seem to be systematically more metal poor than this value thus indicating a possible zero point difference of the order of 0.2 dex and comparable to the probable shift between our cluster metallicities and the ones taken from the literature. However, such a difference between cluster and field stars has not been seen in a study by Korn et al. (2000) who employed high resolution spectroscopy of supergiants.

The AMR for stars older than 3 Gyr is consistent with little or even no enrichment until 8 Gyr ago. The AMR in this age range agrees well with the 4 Gyr old clusters studied by Sarajedini (1998) and also ESO 121 SC03 is in agreement with the derived field star AMR, especially when taking the systematic underestimation of the metallicity for older stars on the order of $0.05 - 0.1$ dex into account (see Sect. 3). Therefore, we do not see the necessity that ESO 121 SC03 belongs to a dwarf galaxy that is in the process of merging with the LMC as proposed by Bica et al. 1998).

The field population of NGC 1651 and NGC 2257 is considerably different from that around the other clusters: around NGC 1651 we find two distinct field populations, around NGC 2257 only one, thus these fields cannot be compared to the other fields, where a mixture of populations have been detected. These fields contain a significantly larger fraction of old stars than the other fields, what is expected from their location in the LMC (e.g. Santos Jr. et al. 1999).

If cluster and field are compared it becomes apparent that our AMR does not argue for an extremely decoupled enrichment history between cluster and field stars, only hints can be seen that the younger clusters are slightly more metal poor than the surrounding field population of the same age. Bica et al. (1998) found the same behaviour for several of their (young) clusters and the surrounding field population. One has to consider the possibility, that these low mean cluster abundances are a result of the statistically larger effect of blending towards the cluster. This has been proposed by Bessell (1993) to explain the low Strömgren metallicity of NGC 330 measured by Grebel & Richtler (1992). In this work of Grebel & Richtler (1992) the mean metallicity found for the surrounding field population

Table 4. Results for the 5 clusters investigated in this work. The error includes the calibration uncertainty.

Cluster	E_{B-V}	Metallicity [dex]	log(Age [y])	Remarks
NGC 1651	0.01 to 0.05	-0.65 to -0.45	9.4 to 9.1	reddening problematic
NGC 1711	0.09 ± 0.03	-0.57 ± 0.17	7.7 ± 0.05	reddening of the field is larger
NGC 1806	0.16 ± 0.06	-0.71 ± 0.24	8.7 ± 0.1	
NGC 2031	0.09 ± 0.05	-0.52 ± 0.21	8.2 ± 0.1	
NGC 2136/37	0.09 ± 0.05	-0.55 ± 0.23	8.0 ± 0.1	no differences between the two clusters
NGC 2257	0.04 ± 0.04	-1.63 ± 0.21	10.2 ± 0.1	

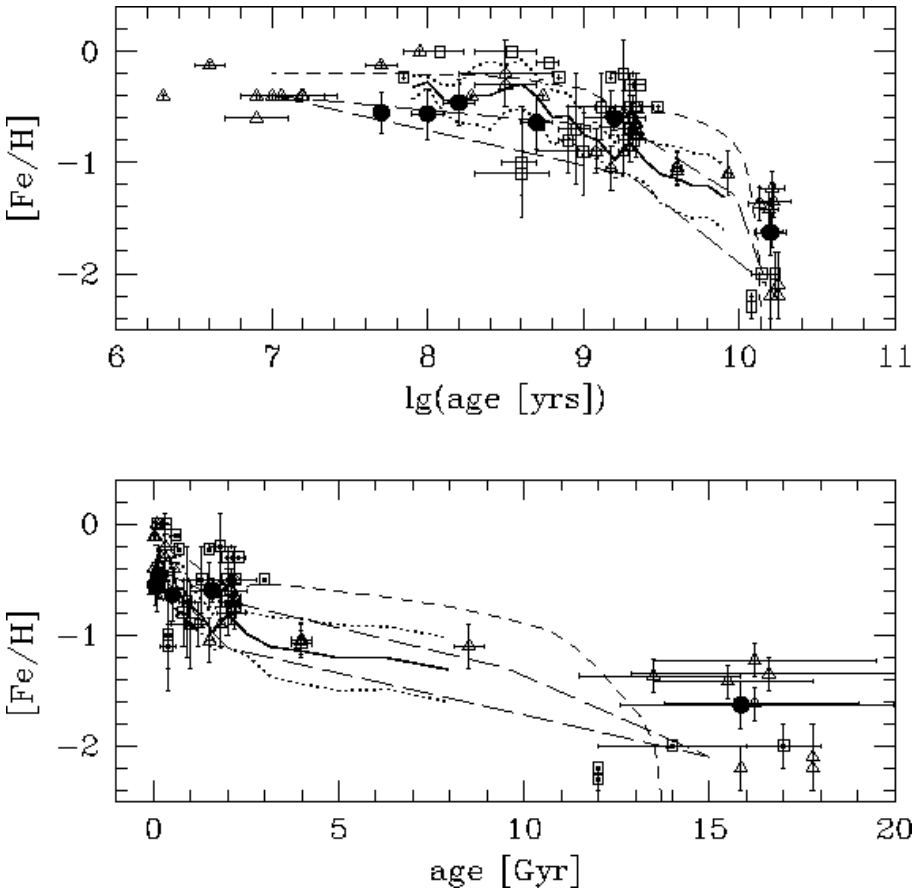

Fig. 32. Published ages and metallicities for LMC clusters, given in TableA5 (open triangles) and in the compilation by Sagar & Pandey (1989) with a limiting magnitude of fainter than $V = 20$ (open squares). The cluster data from this investigation are marked with solid circles. The solid line connects the points in our derived AMR for the field population. The dotted line surrounding the solid line marks the standard deviation of the metallicity around a given age. In addition three models for the AMR are plotted: Pagel & Tautvaišvienė (1998) as short dashed line and two models calculated by Geha et al. (1998) as long dashed line.

(-0.74 dex) agreed well with later on performed spectroscopic measurements (-0.69 dex, Hill 1999) (for a more comprehensive discussion on NGC 330 the reader is referred to the work by Gonzalez & Wallerstein 1999). Having this agreement in mind, one can estimate from the difference of mean field and cluster metallicity that the contamination has a minor effect on our derived metallicities, accounting possibly for a systematic deviation of less than < 0.15 dex.

Our AMR is inconsistent with a recent calculation presented by Pagel & Tautvaišvienė (1998) based on LMC clusters and on planetary nebulae observed by Dopita et al. (1997), that predicts a steeper increase of the metallicity in earlier time, thus older stars should have a higher metallicity than what we observe (see Fig. 32). The AMR is more consistent with closed box model calculations performed by Geha et al. (1998). They present theoretical enrichment models for the two SFHs put forward by Holtzman et al. (1997) and by Vallenari et al. (1996a,b). These SFHs agree in the sense, that a long period of low star formation activity was followed by a sudden increase about 2 Gyr ago. With the Vallenari et al.- SFH, the metallicity increased by a factor of five during the last 2 Gyr, while a modest increase of a factor of three resulted from the Holtzman et al.-SFH.

Dopita et al. (1997) published an AMR for the LMC based on planetary nebulae and found that the metallicity only doubled in the last 2-3 Gyr which is seen in our AMR as well. Another common feature is that a distinct enrichment (if any) between 4 and 9 Gyr cannot be seen. A comparison of the Dopita et al.-values with ours is made difficult by the fact that they measured α-element abundances instead of $[Fe/H]$, but they stated that *"there is no evidence in this sample of any "halo" abundance object"*. If we would apply a constant shift of -0.35

on the [O/H]-abundance, to correct approximately the [O/Fe] overabundance in the LMC in comparison to the Milky Way the metallicity of the PNs with an age of $10^{8.8} - 10^{9.8}$ yr would nicely be in coincidence with our measurements. However, the $[O/Fe]$ variation in dependence of $[Fe/O]$ is still under discussion (see e.g. Russell & Dopita 1992 or Pagel & Tautvaišvienė 1998).

Judging from the field around NGC 2257 we find that no radial metallicity gradient can be seen, since the field stars are consistent with the AMR derived from the inner fields. Taking also NGC 1651 into account we find that in fields where no recent star formation happened the stellar population is dominated by a population with an age between 2 and 4 Gyr. Thus deriving a global SFH on a limited sample is quite uncertain.

15.1.1. The Star Formation History

The manner in which we derived the field star SFH contains several points that may induce biases. One reason is that the isochrones have only a crude spacing in the parameters age and metallicity. Therefore, simulations are helpful for a discussion of the SFH of the field population as described above (Sect. 12). To derive a SFH from our data is more difficult than to derive an AMR, since one has to know not only the age of a star with a given metallicity, but the amount of stars with a given age has to be quite precise. As a result the AMR is quite robust against for example reddening variations compared to the AND.

Two SFHs are shown that illustrate how to interpret the AND (Fig. 33). One SFH has a constant SFR during the whole LMC evolution and thus serves to give an impression how the selection effects behave (left two panels in Fig. 33).The SFR of the second SFH was constant until $10^{9.7}$ yr ago, then it increased by a factor of 5 until $10^{8.4}$ yr ago, before the SFR dropped to its old low level. The AND & AMR resulting from this SFH is plotted in the right panel of Fig. 33.

The constant SFR is marginally inconsistent with our data, which holds for a different reddening correction of $E_{b-y} = \pm 0.02$. This is not true for exact behaviour of the SFH: for example a decrease in the reddening of $E_{B-V} = 0.02$ results in a SFH in which a much larger increase (around a factor of 10) is necessary to describe the observations. However, the general trend, namely, the increase of the SFR around $10^{9.5\pm0.2}$ yr ($2 - 5$ Gyr) ago and the necessary declining SFR some $10^{8.5}$ yr ago in these fields is more robust. Since stars in the LMC should be mixed (at least azimuthally) after $\approx$ 1 Gyr (Gallager et al. 1996) the SFH of the older stars should be a measure for the average SFH of the LMC in the radial distance of the investigated clusters. As a rule of thumb an increase in the applied reddening correction of $E_{b-y} = 0.1$ results for a single age population in a decrease in age by a factor of 0.7.

Vallenari et al. (1996a,b) proposed, on the basis of ground based observations, a SFH in which the SFR increased about a factor of ten 2 Gyr ago, thus only around 5 % of the stars should be older than 4 Gyr. This has recently also been found by Elson et al. (1997) with HST observations. A different SFH was advanced by Holtzman et al. (1997), Geha et al. (1998) and Holtzman et al. (1999) also based on HST observations. In their model, approximately half of the stars are older than 4 Gyr. In our data the fraction of stars older than 4 Gyr is 40 ± 20%, but we note that already a small additional reddening of of $E_{b-y} = 0.015$ leaves only $\approx$ 15% of the stars older than 4 Gyr. Olsen (1999) used Washington photometry of the LMC field population and derived a SFH which is compatible with the one proposed by Holtzman et al. (1999).

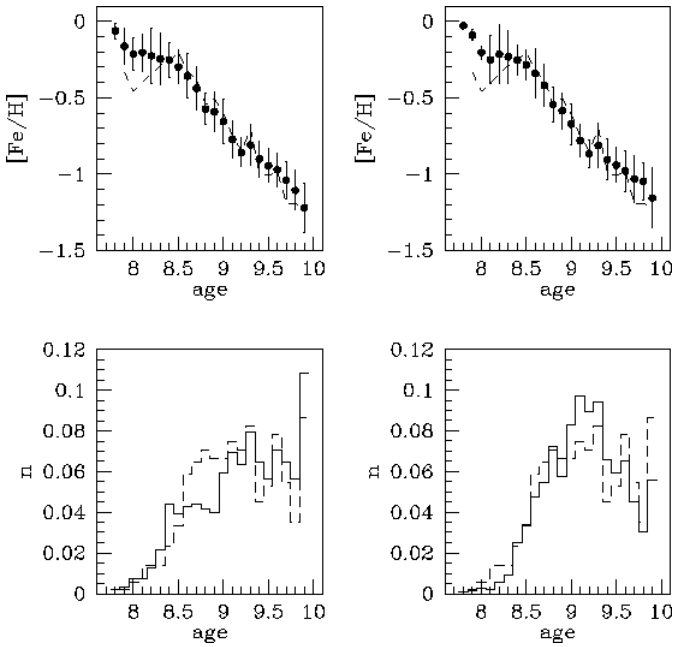

Fig. 33. Simulation with a quasi continuous SFR. The left panel shows the AMR and AND for a constant SFR over the last 10 Gyr. In the right graph the symbols and solid line correspond to a SFH which was constant until $10^{9.7}$ yr, at $10^{9.6}$ yr it increased by a factor of 4 until $10^{8.6}$ yr ago after that the SFR dropped to the same level as in the beginning. The dashed line shows the result of our composite field.

Summarizing, despite the uncertainty in the amount of the increase, the SFH is consistent with an increased SFR that started roughly 3 ± 1 Gyr ago. Interestingly the sparsely populated outer fields are tentatively populated by mainly a population with ages between 2 and 4 Gyr. If this result will hold for a larger sample of outlying fields this could mean that the stellar body of the inner part of the LMC contains more younger *and* older stars compared to these intermediate age stars than the more remote parts of this galaxy. However, spectroscopic studies of several of these candidate stars are needed, especially because the tilted red clump of NGC 1651 could be due to a He overabundance and thus isochrones might be misleading.

The observed SFH is inconsistent with a starformation history in which no star has been born between 4 and 8 Gyr. The simulations showed that virtually no star should have been recovered with an age of more than $10^{9.3}$ yr, even if the differential reddening is as large as $E_{B-V} = 0.07$ and the binary fraction is 70%. However, a large amount of old (> 10 Gyr) CN anomal stars could mimic starformation between 4 and 8 Gyr.

A last remark on the cluster formation rate: it has been noted several times that there apparently was a long period in the LMC where no clusters (or a few) have been formed. Recently, Larsen & Richtler (1999) performed a search for bright star clusters in 21 face-on galaxies. They found a correlation of the specific cluster frequency with parameters indicating the SFR. The age gap of the LMC cluster thus could reflect the low SFR during this period, where the condition for cluster formation where not present.

16. Summary

We tried to determine the Age Metallicity Relation (AMR) and the Star Formation History (SFH) in the LMC on the basis of metallicities and ages of red giants, measured by Strömgren photometry. Our stars are located both in star clusters and in the respective surrounding fields. While statements regarding the AMR are relatively robust, the SFH is much more difficult to evaluate because of the incompleteness effects, for which we can only approximately correct.

Between 8 to 3 Gyr ago the metallicity of the LMC was constant or varied only very slow, after this period the speed of the rate of the enrichment grew: starting 3 Gyr ago the metallicity of the stars increased by a factor of six. The cluster and field AMR during this time was coupled, however a possibility remains that the cluster have on the average a slightly smaller metallicity than the field stars of the same age. Our field star AMR is also consistent with the 4 Gyr old clusters recently studied by Sarajedini (1998) and with ESO 121 SC03. Thus for the latter there is no need to explain this cluster as a recent merger remnant. Good agreement can be found with the photometrically determined metallicity of the young stars and the abundances measured with high resolution spectroscopy. The star formation rate increased around 3 Gyr ago, however it is not possible to constrain the SFH further due to uncertainties in reddening, the CN anomaly and the difficult completeness considerations.

Acknowledgements. The authors gratefully acknowledge observing time at La Silla and the aid by the staff of the European Southern Observatory. We are grateful to E. Grebel and J. Roberts for the opportunity to use their isochrones. We thank the referee for his/her comments and suggestions which greatly helped to improve the paper. We also thank Doug Geisler and Antonella Vallenari for their valuable comments. BD was supported through the DFG Graduiertenkolleg "The Magellanic Clouds and other dwarf galaxies" (GRK 118). MH thanks Fondecyt Chile for support through 'Proyecto FONDECYT 3980032'. WPG gratefully acknowledges support received by Fondecyt grant No. 1971076. TR thanks the Uttar Pradesh State Observatory, Nainital, for warm hospitality and financial support. This research has made use of the Simbad database, operated at CDS, Strasbourg, France.

Appendix A: Appendix

Table A1. Observing log

Object	Filter	Night	Exposure time	Seeing
NGC 1711	y	8.1.94	300 sec	1.4"
	y	8.1.94	300 sec	1.3"
	b	8.1.94	600 sec	1.2"
	b	8.1.94	600 sec	1.3"
	v	8.1.94	900 sec	1.5"
	v	8.1.94	900 sec	1.2"
NGC 1806	y	6.1.94	300 sec	1.1"
	y	6.1.94	300 sec	1.1"
	y	6.1.94	900 sec	1.5"
	b	6.1.94	900 sec	1.1"
	y	7.1.94	600 sec	1.0"
	v	7.1.94	1200 sec	1.1"
	b	7.1.94	900 sec	1.0"
	y	8.1.94	600 sec	1.3"
	b	8.1.94	900 sec	1.2"
	v	8.1.94	900 sec	1.3"
	v	8.1.94	900 sec	1.3"
NGC 1651	y	6.1.94	300 sec	1.4"
	y	6.1.94	600 sec	1.1"
	b	6.1.94	1200 sec	1.1"
	v	6.1.94	1200 sec	1.2"
	v	6.1.94	1200 sec	1.1"
	y	7.1.94	600 sec	0.9"
	b	7.1.94	1200 sec	1.0"
	v	7.1.94	1200 sec	1.0"
	v	7.1.94	1200 sec	1.0"
NGC 2031	y	12.11.92	300 sec	1.1"
	b	12.11.92	600 sec	1.3"
	v	12.11.92	240 sec	1.3"
	v	12.11.92	1200 sec	1.2"
	y	14.11.92	600 sec	1.2"
	y	14.11.92	120 sec	1.4"
	b	14.11.92	120 sec	1.3"
	b	14.11.92	400 sec	1.1"
	v	14.11.92	240 sec	1.4"
	v	14.11.92	1140 sec	1.3"
NGC 2136/37	y	12.11.92	120 sec	1.1"
	b	12.11.92	120 sec	1.5"
	v	12.11.92	120 sec	1.1"
	y	13.11.92	600 sec	1.2"
	b	13.11.92	900 sec	1.2"
	v	13.11.92	1200 sec	1.2"
NGC 2257	v	6.1.94	1200 sec	1.2"
	v	6.1.94	600 sec	1.2"
	b	6.1.94	600 sec	1.2"
	y	6.1.94	300 sec	1.2"
	y	7.1.94	600 sec	1.1"
	b	7.1.94	900 sec	1.1"
	b	8.1.94	300 sec	1.0"
	b	8.1.94	300 sec	1.0"
	b	8.1.94	300 sec	1.0"
	y	8.1.94	300 sec	1.4"
	y	8.1.94	600 sec	1.1"
	v	8.1.94	900 sec	1.2"
	v	8.1.94	900 sec	1.2"

References

Andersen M.J., Freyhammer L., Storm J., 1995, Technical Reports on the 1.54m Telescope, www.ls.eso.org/lasilla/Telescopes/2p2T/D1p5M/RepsFinal/

Ardeberg A., Gustafsson B., Linde P., et al. 1997, A&A 322, L13

Barbaro, G., Olivi F.M., 1991, AJ 101, 922

Beaulieu J.-P., Sackett P.D., 1998 AJ 116, 209

Bell R.A., Gustafsson B., 1978, A&AS 34, 229

Bencivenni D., Brocato E., Buonanno R., et al., 1991, AJ 102, 137

Bertelli G., Bressan A., Chiosi C., et al., 1994, A&AS 106, 275

Bessell M.S., 1993, In New Aspects of Magellanic Cloud research, Springer Berlin Heidelberg, ed Baschek B., Klare G., Lequeux J., p. 321

Bhatia R., Piotto G., 1994, A&A 283, 424

Table A2. The age of NGC 1711 given in the literature.

Author	Age	Method
Cassatella et al. 1996	$10^{7.41}$ yr	UV spectra
Girardi et al. 1995	$10^{7.58}$ yr	M_V of MSTO
	$10^{7.99}$ yr	M_V of CHeB stars
Barbaro & Olivi 1991	$10^{7.57}$	UV colours
Sagar & Richtler 1991	$10^{7.18}$ yr	Isochrones
Mateo 1988	$10^{7.7}$ yr	Isochrones

Table A3. The derived AMR for all field stars around the investigated clusters.

log(age [y])	Metallicity	standard deviation of metallicities	number of stars
7.9	-0.26	0.11	2
8.0	-0.27	0.04	3
8.1	-0.43	0.16	5
8.2	-0.47	0.17	8
8.3	-0.39	0.26	10
8.4	-0.40	0.30	18
8.5	-0.33	0.21	25
8.6	-0.29	0.22	30
8.7	-0.41	0.19	47
8.8	-0.59	0.25	52
8.9	-0.58	0.20	52
9.0	-0.74	0.19	48
9.1	-0.81	0.15	46
9.2	-0.98	0.16	41
9.3	-0.82	0.30	54
9.4	-0.99	0.19	33
9.5	-1.11	0.28	27
9.6	-1.15	0.29	42
9.7	-1.21	0.31	30
9.8	-1.31	0.33	25
9.9	-1.31	0.27	46

Table A4. Metallcity measurements of LMC field stars with high resolution spectroscopy.

Sample and size	[Fe/H][2]	Reference
SG/Cepheids - 7	-0.37	Luck & Lambert 1992
SG - 8	$-0.47/-0.33$	Russell & Bessell 1989
SG - 6	$-0.51/-0.29$	Mc William & Williams 1990
SG - 9	-0.27	Hill et al. 1995
SG - 2	-0.42[1]	Jüttner et al. 1993
SG - 1	-0.3[1]	Fry & Aller 1975
SG - 2	-0.5[1]	Korn et al. 2000

SG stands for supergiants.
[1] transformed to a solar iron abundance of 7.50. [2] If two values are given, the first was derived with the Fe I line the second with the Fe II line. The stars measured by different authors are not always different stars: for example for 4 stars in the list of Mc William & Williams (1990) also Hill et al. 1995 obtained a metallicity. We nevertheless use a simple mean for the mean field star abundance in our paper.

Bica E., Clariá J. J., Dottori, H., et al., 1996, ApJS 102, 57
Bica E., Geisler D., Dottori H., et al., 1998, AJ 116, 723
Binney J., Merrifield M., 1998, Galactic Astronomy, Princeton University Press, Princeton, New Jersey, p. 347
Bomans D.J., Vallenari A., de Boer K.S., 1995, A&A 298, 427
Brocato E., Castellani V., Ferraro F.R., et al., 1996, MNRAS 282, 614
Burstein A., Heiles C., 1982, AJ 87, 1165
Cassatella A., Barbero J., Geyer E.H., 1987, ApJS 64, 83
Cassatella A., Barbero J., Brocato E., et al., 1996, A&A 306, 125
Cayrel de Strobel G., Soubiran C., Friel E.D., et al., 1997, A&AS 124, 299
Crawford D.L., Barnes J.V., 1970, AJ 75, 978
Dieball A., Grebel E.K., 1998, A&A 339, 773
Dolphin A.E., Hunter D.A., 1998, AJ 116, 1275
Dopita M.A., Vassiliadis E., Wood P. R., et al., 1997, ApJ 474, 188
Elson R.A.W., Fall S.M., Freeman K.C., 1987, ApJ 323, 54
Elson R.A.W., Gilmore G.F., Santiago B.X., 1997, MNRAS 289, 157
Frogel J.A., Blanco V.M., 1990, ApJ 365, 168
Fry M.A., Aller L.H., 1975, ApJS 29, 55
Gallagher J.S., Mould J.R., de Feijter E., 1996, ApJ 466, 732
Geha M.C., Holtzman J.A., Mould J.R., et al., 1998, AJ 115, 1045
Geisler D., Bica E., Dottori H., et al., 1997, AJ 114, 1920
Gieren W.P., Richtler T., Hilker M., 1994, ApJ 433, L73
Gieren W.P., Fouqué P., Gómez M., 1998, ApJ 496, 17
Gilmozzi R., Kinney E.K., Ewald S.P., et al., 1994, ApJ 435, L43
Girardi L., 1999, astro-ph/9907086
Girardi L., Chiosi C., Bertelli G., et al., 1995, A&A 298, 87
Gonzalez G., Wallerstein G., 1999, AJ 117, 2286
Grebel E.K., Richtler T., 1992, A&A 253, 359
Grebel E.K., Roberts W.J., 1995a, AAS 186, 0308
Grebel E.K., Roberts W.J., 1995b, A&AS 109, 293
Gustafsson B., Bell R.A., 1979, A&A 74, 313
Hilker M., 1999, astro-ph/9911387
Hilker M., Richtler T., Stein D., 1995a, A&A 299, L37
Hilker M., Richtler T., Gieren W.P., 1995b, A&A 294, 37
Hill V., 1999, A&A 345, 430
Hill V., Andrievsky S., Spite M., 1995, A&A 293, 347
Hill R.S., Cheng K.P., Bohlin R.C., et al., 1995, ApJ 446, 622
Holtzman J.A., Mould J.R., Gallagher J.S. III, et al., 1997, AJ 113, 656
Holtzman J.A., Gallagher III J.S., Cole A.A., et al., 1999, astro-ph/9907259
Hunter D.A., Shaya E.J., Holtzman J.A., et al., 1995, ApJ 448, 179
Ivans I.I., Sneden C., Kraft R.P., et al., 1999, astro-ph9905370
Jasniewicz G., Thévenin F., 1994, A&A 282, 717
Johnson J.A., Bolte M., Stetson P.B., et al., 1999, ApJ 527, 199
Jønch-Sørensen H., 1993, A&A 102, 637
Jüttner A., Stahl O., Wolf B. et al., 1993 In New Aspects of Magellanic Cloud research, Springer, Berlin Heidelberg, ed. Baschek B., Klare G., Lequeux J., p.337
Kontizias M., Kontizias E., Michalitsiano A.G., 1993, A&A 269, 107
Korn A.J., Becker S.R., Gummersbach C.A., et al., 2000, A&A 353, 655
Larsen S.S., Richtler T., 1999, A&A 345, 59
Lee M.G., 1992, ApJ 399, L133
Luck R.E., Lambert D.L., 1992, ApJS 79, 303
Madore B.F., Freedman W.L., 1998, ApJ 492, 110
Mateo M., 1988, ApJ 331, 261
Mateo M., Hodge P., Schommer R.A., 1986, ApJ 311, 113
Mc Gregor P.J., Hyland A.R., 1984 ApJ 277, 149
Mc William A., Williams R.E., 1990, The Magellanic Clouds, IAUS 148, eds. Haynes R., Milne D., p. 391
Meurer G.R., Freeman K.C., Cacciari C., 1990, AJ 99, 1124
Mould J.R., Xystus D.A., Da Costa G.S., 1993, ApJ 408, 108

Mould J.R., Han M., Stetson P.B., Gibson B., et al., 1997, ApJ 483, L41
Oey M.S., Massey P., 1995, ApJ 452, 210
Olsen K.A.G., 1999, AJ 117, 2244
Olsen K.A.G., Hodge P.W., Wilcots E.M., et al., 1997, ApJ 475, 545
Olsen K.A.G., Hodge P.W., Mateo M., et al., 1998, MNRAS 300, 665
Olszewski E.W., Schommer R.A., Suntzeff N.B., et al., 1991, AJ 101, 515
Pagel B.E.J., Tautvaišvienė G., 1998, MNRAS 299, 535
Panagia N., Gilmozzi R., Macchetto F., et al., 1991, ApJ 380, L23
Piatti A.E., Geisler D., Bica E., Clariá J.J., et al., 1999, astro-ph/9909475
Pilachowski C.A., Sneden C., Kraft R.P., et al., 1996, AJ 112, 545
Ratnatunga K.U., Bahcall J.N., 1985, ApJS 59, 63
Reitermann A., Stahl O., Wolf B., Baschek B., 1990, A&A 234, 109
Richter P., Hilker M., Richtler T., 1999, astro-ph/9907200
Richtler T., 1990, A&AS 86, 103
Richtler T., Spite M., Spite F., 1989, A&A 225, 351
Richtler T., Sagar R., 1991, A&A 250, 324
Romaniello M., Panagia N., Scuderi S., 1999, astro-ph/9908144
Russell S.C., Bessell M.S., 1989, ApJS 70, 865
Russell S.C., Dopita M.A., 1992 ApJ 384 , 508
Sagar R., Pandey A.K., 1989, A&AS 79, 407
Sagar R., Richtler T., 1991, A&A 250, 324
Santos Jr., J.,F.C., Piatti A.E., Clariá J.J., et al., 1999, AJ 117, 2841
Santiago B.X., Elson R.A.W., Sigurdsson S., et al. , 1998, MNRAS 295, 860
Sarajedini A., 1994, AJ 107, 618
Sarajedini A., 1998, AJ 116, 738
Schaerer D., Charbonnel C., Meynet G., et al., 1993, A&AS 102, 339
Schlegel D., Finkbeiner D., Davis M., 1998, ApJ 500, 252
Schwering P.B.W., Israel F.P., 1991, A&A 246, 231
Stryker L.L., 1984, ApJS 55, 127
Subramaniam A., Sagar R., 1993 A&A 273, 100
Testa V., Ferraro F.R., Brocato E., et al., 1995, MNRAS 275, 454
Thévenin F., Jasniewicz G., 1992, A&A 266, 85
Vallenari A., Aparicio A., Fagotto F., et al., 1994a, A&A 284, 424
Vallenari A., Aparicio A., Fagotto F., et al., 1994b, A&A 284, 447
Vallenari A., Chiosi C., Bertelli G., et al., 1996a, A&A 309, 367
Vallenari A., Chiosi C., Bertelli G., et al., 1996b, A&A 309, 358
Walker A.R., 1990, AJ 100, 1532
Walker A.R., 1993, AJ 106, 999
Walker A.R., Schommer R.A., Suntzeff N.B., et al., 1993, In New Views of the Magellanic Cloud, IAUS 190, eds. Y.-H. Chu, N.B. Suntzeff, J.E. Hesser, et al., p.341
Westerlund B.E., 1997, The Magellanic Clouds, Cambridge University Press, Cambridge
Will J.-M., Bomans D.J., Vallenari A., et al., 1996, A&A 315,125
Zaritsky D., Lin D.N.C., 1997, AJ 114, 2545

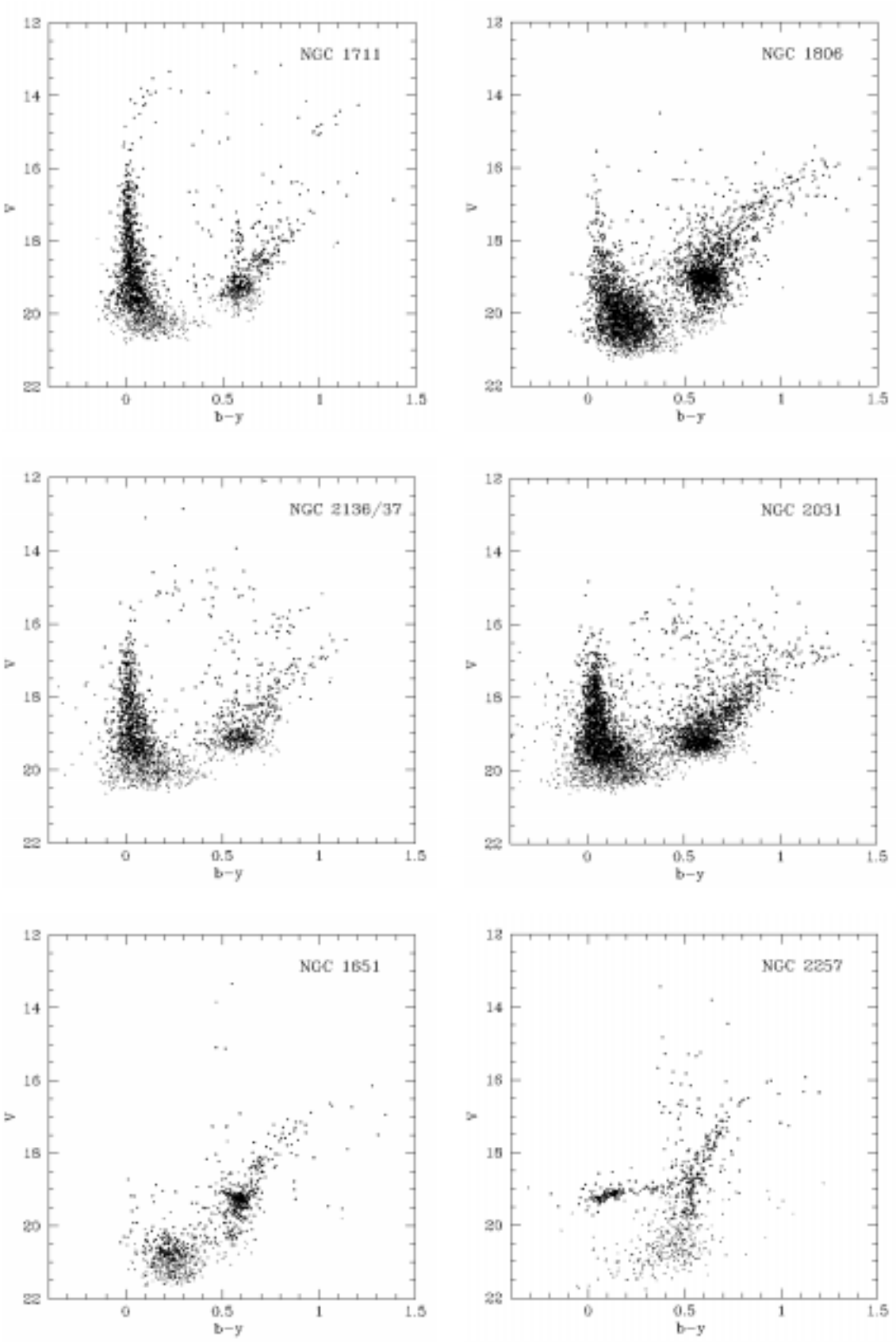

Fig. A1. The CMDs of the whole fields containing the observed clusters. No reddening correction has been applied. The points in bold face are stars with an error $\Delta(b-y) < 0.1$ and $\Delta m1 < 0.1$; the other dots are used for stars found with larger errors.

Table A5. Literature values for age, metallicity and reddening derived or assumed in photometric observations resulting in an CMD.

Cluster	E_{B-V}	$[Fe/H]$	log(Age [y])	Authors
ESO 121-SC03	0.03	-1.1 ± 0.2	9.93 ± 0.01	Bica et al. 1998
R 136	0.38	-0.4	7.0	Hunter et al. 1995
OHSC 33	0.09	-1.05 ± 0.2	9.18 ± 0.03	Bica et al. 1998
OHSC 37	0.15	-0.7 ± 0.2	9.32 ± 0.03	Bica et al. 1998
LH 47/48	0.11	-0.4	6.3	Oey & Massey 1995
LH 52/53		-0.4	7.0	Hill et al. 1995
LH 72	$0 - 0.17$	-0.6	$6.7 - 7.18$ (age spread)	Olsen et al. 1997
LH 77	-0.06 ± 0.01	-0.4	7.20 ± 0.14	Dolphin & Hunter 1998
SL 8	0.04	-0.55 ± 0.2	9.26 ± 0.03	Bica et al. 1998
SL 126	0.01	-0.5 ± 0.2	9.34 ± 0.03	Bica et al. 1998
SL 262	0.00	-0.6 ± 0.2	9.32 ± 0.03	Bica et al. 1998
SL 388	0.03	-0.7 ± 0.2	9.34 ± 0.03	Bica et al. 1998
SL 451	0.1	-0.75 ± 0.2	9.34 ± 0.03	Bica et al. 1998
SL 503	0.04 ± 0.01	-0.4	7.20 ± 0.22	Dolphin & Hunter 1998
SL 509	0.03	-0.9	9.08	Bica et al. 1998
SL 663		-1.05 ± 0.16	9.60 ± 0.03	Sarajedini 1998
SL 817	0.07	-0.55 ± 0.2	9.18 ± 0.03	Bica et al. 1998
SL 842	0.03	-0.65 ± 0.2	9.34 ± 0.03	Bica et al. 1998
SL 862	0.09	-0.9 ± 0.2	9.26 ± 0.03	Bica et al. 1998
NGC 1711	0.09	0	7.8	Richtler & Sagar 1991
NGC 1754	0.09 ± 0.02	$-1.42 \pm 0.15 (-1.54^a)$	10.19 ± 0.06	Olsen et al. 1998
NGC 1786	0.09 ± 0.05	-2.1 ± 0.3	as old as M68	Brocato et al. 1996
NGC 1835	0.08 ± 0.02	$-1.62 \pm 0.15 (-1.72^a)$	10.21 ± 0.07	Olsen et al. 1998
NGC 1841	0.20 ± 0.03	-2.2 ± 0.2	as old as M68	Brocato et al. 1996
	0.18 ± 0.02	-2.3 ± 0.4	as old as M92	Walker 1990
NGC 1848	0.2 [3]	-0.4	$6.7 - 7.0$	Will et al. 1996
NGC 1850A	0.18 ± 0.02	-0.12 ± 0.03 [1]	7.7 ± 0.1	Gilmozzi et al. 1994
	0.18	-0.4	7.7 ± 0.1	Vallenari et al. 1994b
NGC 1850B	0.18 ± 0.02	-0.12 ± 0.03 [1]	6.6 ± 0.1	Gilmozzi et al. 1994
	0.18	-0.4	7.0	Vallenari et al. 1994b
NGC 1858	0.15	-0.4	6.9	Vallenari et al. 1994b
NGC 1866	0.03	-0.43 ± 0.18	8	Hilker et al. 1995b
NGC 1898	0.07 ± 0.02	$-1.37 \pm 0.15 (-1.37^a)$	10.13 ± 0.07	Olsen et al. 1998
NGC 1955	0.09 ± 0.01	-0.4	7.19 ± 0.15	Dolphin & Hunter 1998
NGC 1978	0.08	-0.4	9.34	Bomans et al. 1995
NGC 2004	0.07 ± 0.01	-0.4	7.19 ± 0.15	Dolphin & Hunter 1998
	0.06	0	6.9	Benicivenni et al. 1991
NGC 2005	0.1 ± 0.02	$-1.35 \pm 0.15 (-1.92^a)$	10.22 ± 0.11	Olsen et al. 1998
NGC 2019	0.06 ± 0.02	$-1.23 \pm 0.15 (-1.81^a)$	10.21 ± 0.08	Olsen et al. 1998
NGC 2027	0.05 ± 0.01	-0.4	7.06 ± 0.14	Dolphin & Hunter 1998
NGC 2121		-1.04 ± 0.13	9.60 ± 0.03	Sarajedini 1998
NGC 2134	0.22	-0.4	8.28	Vallenari et al. 1994a
NGC 2155		-1.08 ± 0.12	9.60 ± 0.03	Sarajedini 1998
NGC 2164	0.10	0--0.4	8	Richtler & Sagar 1991
NGC 2210	0.09 ± 0.03	-2.2 ± 0.2	as old as M68	Brocato et al. 1996
NGC 2214	0.07	0	7.95	Bhatia & Piotto 1994
		0	7.78 ± 0.1	Lee 1992
	0.07	0--0.4	8	Richtler & Sagar 1991
NGC 2249	0.25	-0.4	8.74	Vallenari et al. 1994a

We collected literature which has been published after the work by Sagar & Pandey (1989). The metallicities are in several cases from other sources: [1] Jasniewicz & Thevenin (1994), [2] Olszewski et al. (1991), [3] Schwering & Israel (1991). [a] The authors quote two values for the cluster, one derived with the method by Sarajedini (1994) and one obtained earlier by Olszewski et al. (1991); the authors prefer the photometrically determined metallicities and thus only ages according to these metallicities are stated.